Politecnico di Torino

Aalto-yliopisto
Aalto-universitetet
Aalto University

Master's degree in Mechanical Engineering

A.a. 2025/2026

Graduation Session 03/2026

Role of the HVAC system to promote good air quality conditions on passenger vessels

Supervisors:
ELIODORO CHIAVAZZO
HEIDI SALONEN

Advisor:
KUJALA PENTTI

Candidate:
GAETANO FRANCESCO
MACALUSO

Abstract

Ensuring good indoor air quality (IAQ) on passenger ships has become an increasingly important challenge, especially after the COVID-19 pandemic which showed the weaknesses of onboard HVAC systems in managing airborne pathogen spread. This thesis examines the role of air purification measures in enhancing indoor air quality (IAQ) on cruise ships, focusing specifically on the integration of emerging technologies within HVAC networks. The research is conducted in collaboration with Halton Oy, a worldwide supplier of marine HVAC systems, and AirForte Oy, a Finnish manufacturer of advanced solutions for air cleaning. A comprehensive state of the art review is conducted to to evaluate conventional purification technologies, such as mechanical filtration systems (HEPA, ULPA, EPA), UVGI disinfection systems, photocatalytic oxidation, and ionization systems. Their benefits, limitations, and technical aspects like pressure drop, maintenance, and spatial constraints are discussed thoroughly. As a reference case study, a Helsinki–Stockholm passenger ship is taken into consideration for the installation and analysis of the AirForte Aero Quattro air purification technology, specifically within the Sunflower Pool Area, a confined recreational facility with high humidity and variable occupancy. Two theoretical setups using only HEPA filtration and only UVGI disinfection are also examined by modeling and simulations under idealized duct conditions with reference airflow data, allowing for a comparative assessment of the three technologies. By using analytical calculations and system modeling, every solution is evaluated against air cleaning efficiency, installation volume required, pressure losses, energy performance, and maintenance implications. Results show that although conventional solutions like HEPA and UVGI exhibit high particle removal and pathogen inactivation efficiency, they have some limitations in their operations. The AirForte system, on the other hand, works just as well at cleaning air, but with less pressure drop, no ozone production, and less maintenance. This makes it a good choice for use on ships.

The results of this research have important implications for naval architects, HVAC engineers, and public health practitioners seeking to improve airborne infection control on passenger ships, with a view to developing a safer and more sustainable maritime domain.

Acknowledgements

I would like to express my deepest gratitude to both Aalto University and the Politecnico di Torino for providing me with invaluable academic support and guidance throughout my entire study path and during the development of this thesis project. I am sincerely thankful to Halton Oy and Airforte Oy for their technical assistance and for providing the educational material that made this research possible.

In particular, I wish to express my heartfelt appreciation to Professor Pentti Kujala from Aalto University, for his continuous guidance, insightful advice, and support during the writing of this thesis and throughout the meetings with Halton and Airforte.

A special thanks goes to Mr. Mika Kirjavainen from Halton Oy for sharing his deep professional expertise and experience in the field of HVAC systems, which has been essential for the progress of my work. I am also grateful to Airforte Oy, in particular to Mr. Markus Lankinen and Mr. Kai Vuori, for their technical support and for providing study materials related to their Aero Quattro technology, which significantly enriched my research.

I would also like to extend my sincere thanks to Professor Heidi Salonen, my supervisor at Aalto University, for her continuous encouragement and valuable feedback throughout the thesis process, and to Professor Eliodoro Chiavazzo from the Politecnico di Torino for his kind support and guidance during the development of this work.

Finally, I wish to thank all those who, directly or indirectly, have contributed to the completion of this thesis with their support and inspiration.

Table of Contents

List of Tables VI

List of Figures VII

1 Introduction 1
- 1.1 Background and Problem Statement . . . 1
- 1.2 Objectives and Scope of the study . . . 2
- 1.3 Structure of the thesis . . . 3

2 State of the Art 6
- 2.1 Introduction to Indoor Air Quality on Passenger Ships . . . 6
- 2.2 Mechanical filtration system . . . 8
  - 2.2.1 Air Filter Classification Systems: ISO 16890, MERV and EN 779 . . . 9
  - 2.2.2 High Efficiency Particle Filters . . . 10
- 2.3 UVGI System . . . 12
  - 2.3.1 Effectiveness of the System . . . 13
  - 2.3.2 Low Pressure Mercury Vapor Lamps . . . 14
  - 2.3.3 UV-C LEDS . . . 16
  - 2.3.4 UV Photocatalytic Oxidation . . . 17
  - 2.3.5 Maintenance and Safety Precautions . . . 18
- 2.4 Ionization Based Air Purification Technology . . . 19

3 Case Study: Passenger Vessel 21
- 3.1 Ship Overview . . . 22
  - 3.1.1 General Description . . . 22
  - 3.1.2 Capacity and Operational Profile . . . 24
  - 3.1.3 Ship's HVAC System Overview . . . 25
- 3.2 Selected Test Area: Sunflower Oasis . . . 25
  - 3.2.1 Current HVAC system: AC232 . . . 29

4 Theoretical Case Study Calculations 32
4.1 Introduction . . . 32
4.1.1 Purpose and Scope of the Study . . . 32
4.1.2 Characteristics and Operational Parameters of the Theoretical Case Study . . . 34
4.2 Case A: HEPA Filtration System . . . 35
4.2.1 System Configuration . . . 35
4.2.2 Clean Air Delivey Rate (CADR) . . . 36
4.2.3 Pressure Drop . . . 37
4.2.4 Decay Time of Particles . . . 40
4.2.5 Maintenance Considerations . . . 41
4.3 Case B: UVGI Purification System . . . 44
4.3.1 System Configuration . . . 44
4.3.2 System settings . . . 45
4.3.3 Survival Fraction of Microbial Population Exposed to UV-C Energy . . . 46
4.4 Decay Time of Particles . . . 50
4.5 Eneergy Analysis . . . 51
4.5.1 Maintenance Considerations . . . 52

5 Aero Quattro AirForte Technology 54
5.1 System's Description . . . 54
5.2 Experimental Performance of the Aero Quattro Technology . . . 57
5.2.1 Experimental Procedure . . . 58
5.2.2 Virological Results . . . 58
5.3 Aero Quattro Technology and Theoretical Case Comparison . . . 59
5.4 Integration of Aero Quattro Units: Space Analysis and Configuration of AC room 25 . . . 61

6 Conclusions and Perspectives 63
6.1 Critical Reflection and Future Evolution of the Research . . . 64
6.2 Aspects Requiring Further Investigation . . . 66
6.3 Concluding Perspectives . . . 66

Bibliography 67

List of Tables

4.1 Assumed parameter values for theoretical pressure drop calculation 40

List of Figures

2.1 Particles size comparison. Adopted from DNV, Aerosol Distribution and Transmission Supported by Ventilation Systems (2021). 7

2.2 Different particle filtrations. Top left: Straining. Top right: Impingement. Bottom left: Interception. Bottom right: Diffusion. Adopted by Heinen and Hopman, white paper (2020). 8

2.3 Air Filter Efficiency Classification. Adapted from Airguard Envirocare est. (1985). 10

2.4 Structure of a HEPA filter. Source: Wikipedia (accessed 12 March 2025) 11

2.5 Filter groups. (Adopted from Heinen and Hopman, white paper, 2020) 12

2.6 Ultraviolet light spectrum. Source: Wikipedia (accessed 12 March 2025). 13

2.7 Low Pressure Mercury Lamps. Source: Jelight Company Inc. Official website. Available at: https://www.jelight.com/low-pressure-mercury-lamps/ (accessed 6 April 2025). 15

2.8 Low Pressure Mercury Lamp Output as Function of Cold-Spot Temperature. Source: ASHRAE Handbook – HVAC Systems and Equipment, 2024. 16

2.9 UV-C Led lamps. Adopted from Halton Oy study material. 17

2.10 Ionization process. Adopted from AirForte Oy study material. . . . 19

3.1 Example of a modern passenger vessel, representative of the type of ships considered in this study. Adopted from Quality travel's website. Available at: https://www.qualitytravel.it/grandi-navi-veloci-festeggia-unestate-da-record-ai-gnv-awards/115367 (accessed 10 April 2025). 22

3.2 Reference passenger vessel deck's plan. Adapted from NaParome website. Avaiable at: https://symphony-silja.narod.ru/.(accessed 10 April 2025). 23

3.3 All ferry routes operated by Tallink Silja Line between Finland, Sweden, Estonia, Latvia, and the Åland Islands. Adopted from Tallink Group official website. Avaiable at: https://www.tallink.com/ (accessed 11 April 2025 24
3.4 Sunflower Oasis Pool Area. Adopted from Tallink Group official website. Avaiable at: https://www.tallink.com/on-board/spas-saunas (accessed 11 April 2025 26
3.5 Technical ventilation layout of the Sunflower Pool Area (AC232), located on Deck 12 of the reference passenger vessel. The figure shows where the supply air grilles and exhaust air grilles are located. There are specific extraction points near the three main pools to control humidity and make sure the air is always fresh. Image adapted from the vessel's HVAC documentation. 27
3.6 Left-side whirlpool 28
3.7 Right-side whirlpool 28
3.8 HVAC system AC232 serving the Sunflower Pool Area on Deck 12. 29
3.9 Standard HVAC summer case configuration with control volumes C and D (Pre-heater and Humidifiyer) being bypassed due to the summer case operational mode. 31

4.1 Particle concentration decay over the three time periods considered ($t = 0.5h$, $t = 1h$, $t = 1.5h$). 42
4.2 Schematic representation of a typical HVAC system with integrated UVGI disinfection unit. Source: Halton Oy study material. 44
4.3 UV rate constants for coronavirus (adapted from Luo et al., 2021) . 49

5.1 Internal configuration of the Aero Quattro air purification unit. Adopted from Duplissy (2022). 55
5.2 Aero Quattro internal setup. Adopted from Halton Oy official website. Avaiable at: https://www.halton.com/ (accessed 2 May 2025) 56
5.3 Dimensions of the Aero Quattro device unit. Adopted from Halton technical data sheet. 56
5.4 Frontal view of the ventilation duct in AC Room 25 (Deck 12, reference passenger vessel) 61

Chapter 1

Introduction

1.1 Background and Problem Statement

In recent years, especially following the outbreak of the COVID-19 pandemic, the quality of indoor air on board passenger ships has emerged as a critical aspect of public health. Cruise ships are crowded by nature, and they are made up of a network of enclosed spaces where thousands of people spend long periods of time in small spaces. These conditions make them very likely to catch diseases that spread through the air, especially when HVAC systems are involved in moving dirty air around. In most passenger ships, centralized Air Handling Units or Fan Coil Units ventilate living spaces like cabins, lounges, restaurants, and gyms. These units usually work in recirculation mode. While this practice helps conserve energy by reducing the load on heating and cooling systems, it also presents significant health risks. Usually, up to 70% of the air circulated in these spaces is recirculated air, while only the 30% is fresh air intake. The use of circulated air is generally not recommended, since, without an effective air purification system, it could allow virus particles to spread in the other environments of the ship through the centralized air handling units. However, if recirculation is to be used, special air purification strategies must be implemented to mitigate these risks. They include the use of high efficiency filters capable of capturing small size particles, UV lights to inactivate pathogens within ventilation ducts and the optimization of airflow patterns to reduce stagnation areas and prevent contamination between compartments. In addition, there are rooms such as the galley, toilets, mess rooms, and laundry where recirculation is not allowed, and the risk of viral transmission of viruses is generally low, since these environments are provided with an independent ventilation system with a high air change rate.

Virus transmission can take place in several ways. As stated by the World Health Organization (WHO), the spread of the viruses can occur via direct, indirect

or close contact with infected people. Saliva, respiratory secretions and respiratory droplets are expelled when a person coughs, sneezes or talks, and they can remain suspended in air over long distances and time. These infected respiratory droplets can land on objects and surfaces around the person, causing the non infected person to contract the virus by touching their nose or mouth after touching these objects, or by breathing in those particles. While the WHO[1] states that viruses are mainly transmitted via respiratory droplets caused by the close contact with an infected person, it became evident during the 2019 pandemic that the ventilation and air handling systems contributed to the spread of infectious airborne particles in crowded and enclosed environments, where the filtration system and the air cleaning apparatus where not adequate to mitigate the risk of transmission.

A well known, example that demostrates the spread of airborne viruses through the HVAC system, is the outbreak abroad the Diamond Princess cruise ship in early 2020. Despite passengers being quarantined from the first 10 cases confirmed, the number of contaminated cases raised up to 600 people among the passengers in only two weeks from the start of the outbreak. Studies later revealed that the centralized HVAC system had recirculated virus laden aerosols between cabins, facilitating indirect transmission even in the absence of direct contact.

These observations highlight how the design and operation of onboard HVAC systems can significantly influence the risk of airborne disease transmission, especially in enclosed and crowded environmnent of passenger ships. Inadequate filtration, high levels of of air recirculation rates, and virus carrying particles that remain suspended in the air for long periods can lead to the rapid spread of infections from one area of the ship to others, even without direct contact between individuals.

This situation shows the urgent need to reevaluate existing air quality management practices and create improved solutions for sustaining safe and healthy indoor environments on cruise vessels. For those reasons, this thesis aims to investigate the extent of the problem and to explore technical solutions capable of mitigating airborne health risks in maritime settings.

1.2 Objectives and Scope of the study

The purpose of this study is to investigate and experimentally implement an innovative air purification system developed by the finnish company Airforte Oy, specialized in air cleaning technologies, by integrating it with the HVAC system designed by Halton Group, global technology leader in indoor air solutions for demanding spaces and leading supplier of the marine ventilation solutions. The

[1]World Health Organization

final goal is to identify the performance and feasibility of this combined system on a reference vessel operating, for instance, on the Helsinki - Stockholm route.

Unlike the traditional HVAC systems, that rely primarly on mechanical filtration and ultraviolet radiation to control air quality, the study of this thesis will not be focus on filtering air using high efficiency filters, but rather on cleaning the air through the combination of physical and chemical processes that neutralize contaminants before they can circulate in the different rooms of the vessel through the heating, ventilation and air conditioning systems. Although high efficiency filters are highly effective in particle capture, they are associated with several limitations such as pressure drops within the ducts which reduce energy efficiency, and the need of frequent maintenance and high operational costs due to regular replacement, typically required on a yearly basis or even more frequently under high load conditions. In this context, the collaboration between Halton and Airforte represents an opportunity to give us a new technological solution with respect to the conventional systems adopted previously in the marine industry.

The scope of the thesis includes both theoretical and applied research. From the theoretical side, the study reviews the state of the art in indoor air treatment technologies used in the maritime sector and identifies the technical and practical limits of current filtration based systems. On the experimental side, the work involves the analysis and evaluation of AirForte's air cleaning system installed within the Halton HVAC framework, focusing on their integration, operation, and impact on overall air quality on board on the reference passenger vessel we will take into consideration. Through this research, the thesis aims to define not only the effectiveness of the AirForte solution, but also its potential for wide scale application within the shipping industry, in particular addressing heightened post pandemic air cleanliness demands. The outcome will enhance safer, cleaner, and more efficient passenger ship ventilation systems for both public health and operational shipboard sustainability.

1.3 Structure of the thesis

This thesis is organized into six major chapters, all carefully designed to develop the discussion from an overall context of indoor air quality in passenger ships to a comparative study of various air purification methods. The organization follows a logical sequence, beginning with an overview of the issues that were identified, advancing to an investigation of current solutions, and concluding with an overall assessment of a real case study in parallel with a number of theoretical demonstrations. This organization ensures that inferences that are derived are based on a wide-ranging analysis, combining qualitative observations with quantitative assessments.

Chapter 1 provides background and justification for the study, focusing on the health risks of not treating air properly in marine applications and using important lessons learned from recent global health crises. The study's scope is clearly defined, giving the reader an overall understanding and clarifies the emphasis on implementing an advanced air purification system within a ship's HVAC system.

Chapter 2 provides a description of the most advanced air purification and filtration technologies that are used in marine HVAC units. This section gives a short overview of a thorough study of the issues with indoor air quality on cruise ships. It then goes into detail about traditional mechanical filtration methods, high efficiency particulate air (HEPA) filters, ultraviolet germicidal irradiation (UVGI) systems, ultraviolet photon activated photocatalytic oxidation, and ionization technologies.the State of the Art in air purification and filtration technologies, reviewing the most advanced technologies relevant to air purification and filtration systems used in marine HVAC units. This section summarizes an exhaustive study of the indoor air quality issues faced on cruise ships, thereby leading to a detailed discussion of conventional mechanical filtration methods, high efficiency particulate air (HEPA) filters, ultraviolet germicidal irradiation (UVGI) systems, ultraviolet photon activated photocatalytic oxidation, and ionization technologies. The evaluation of each of these technological methods takes into account their efficacy, operational requirements, and intrinsic limitations in the context of international regulations, thus providing a platform for the evaluation of innovative technologies, which are further probed in this thesis.

Chapter 3 presents the real case study, where a reference passenger vessel on the Helsinki–Stockholm route is selected as the subject of the study. The full description of the ship includes its operational layout, passenger amenities, and the layout of its heating, ventilation, and air conditioning (HVAC) system. The Sunflower Pool Area (Spa complex) is the chosen research location. It is a difficult indoor climate zone with high humidity and changing thermal conditions. The HVAC system that provides air conditioning to this facility (AC232) is fully described, including its parts, how it works in the summer and winter, and how it distributes air. This chapter thus sets the technical and environmental context necessary for an in-depth assessment of the AirForte system performance.

Chapter 4 discusses theoretical calculations specific to the case studies chosen. This section of the thesis places two very different hypothetical systems side by side: one made up only with a HEPA filter and the second with a UVGI system alone. Both are evaluated under the same baseline duct and room parameters in order to provide a neutral performance comparison. In each case, calculations are performed to determine the improvement in indoor air quality (IAQ), spatial requirements, the time needed to achieve the air quality level required, and operational aspects related to airflow, power usage, and maintenance requirements. For the HEPA filter,

specific focus is on the pressure drop caused by the filter and the extra ventilation capacity required to maintain the target air change rates. For the UVGI system, analytical emphasis is on microbial inactivation effectiveness, required exposure times, lamp power ratings, and duct locations. Chapter 4 lays a strong quantitative basis for further comparisons.

Chapter 5 analyzes the Real Case Scenario utilizing an assessment of the AirForte Aero Quattro device. A detailed analysis is presented with regards to the design, installation, and integration of the system into the existing Halton HVAC system, using operational data and technical manuals as primary points of reference. The performance assessment includes metrics relevant to the effectiveness of contaminant removal, effects on airflow dynamics, energy consumption, and maintenance requirements. The low pressure drop characteristic of the AirForte apparatus is a highlighted key operational advantage, allowing system integration without requiring rebalancing or adjustments to the ventilation network.

Chapter 6 is a comparative study and conclusion. This section carefully compares Chapter 4's theoretical results with Chapter 5's empirically outlined performance results. The evaluation involves a discussion of efficiency measures together with spatial issues, integration problems, operational practicability, and sustainability over longer time horizons. A discussion of each methodology's advantages and disadvantages, along with possible outcomes from installing advanced purification units within ship HVAC schema, is also included. The concluding section of this chapter finishes with an overview of this research's importance within marine environmental engineering, as well as recommended future study directions. Against this background, the current dissertation moves from a general exposition of the content of the study to targeted, empirical research, thus ensuring that the conclusions made are robustly anchored in both theoretical models and real world, operational outputs.

Chapter 2

State of the Art

2.1 Introduction to Indoor Air Quality on Passenger Ships

Many studies have shown how the indoor air on passenger ships contains a wide range of contaminants that pose significant health risks on both passengers and crew members. According to Schalm et al. (2023), there are three main categories of air pollutants: Biological, chemical and physical. Among the biological agents there are viruses, airborne bacteria, mold spores and allergens, which can proliferate in the HVAC ducts or moist areas within the ships. The chemical contaminants consists mainly of Volatic Organic Compounds (VOCs), combustion byproducts like NO_2 and CO, and ozone produced by equipment, while physical contaminants include particulate matter, such as PM10, and PM2.5, microplastics and airborne marine aerosols that can be introduced through the external ventilation or can be produced onboard. According to institutions like DNV[1] and ASHRAE[2], droplets containing viral pathogens, such as SARS-CoV-2, generated by coughing or sneezing, have a diameter of about 5 µm and can travel for about 1-2 meters away, while the droplet nuclei, which are the residual solid components left behind after the evaporation of respiratory droplets, are typically smaller than 5 µm, ranging from 0.01 µm to 100 µm, and are capable of remaining airborne for many hours traveling for longer distances through the ventilation systems. As reported by the Healthy Sail Panel (2020)[3], "*It takes about 8 minutes for a 10µ particle to settle 5 feet in still air, while a 1µ particle would take 12 hours to settle 5 feet in still air*", emphasizing

[1]Det Norske Veritas

[2]American Society of Heating, Refrigerating and Air Conditioning Engineers

[3]Recommendations from the Healthy Sail Panel (2020)

the prolonged suspension of smaller aerosol particles, which makes enclosed ship environments particularly vulnerable. This prolonged suspension time, increases the likelihood of inhalation by individuals in the same or adjacent environment. Bad indoor air quality (IAQ) can lead to health problems such as the spread of airborne diseases, allergic reactions, respiratory irritation, and long term effects of being around chemicals like VOCs and fine particulate matter. Crew members may be exposed to the substance for a long time because they spend a lot of time on board, especially in small technical areas where there isn't enough air exchange. Figure 2.1 shows a scale of particles that we want to remove from the HVAC system, from viruses and bacteria to pollen and airborne particles. This helps to show the link between particle size and filtration problems. As shown, many of the most dangerous particles fall below 1 µm, which presents a significant challenge for traditional air filters and ventilation systems.

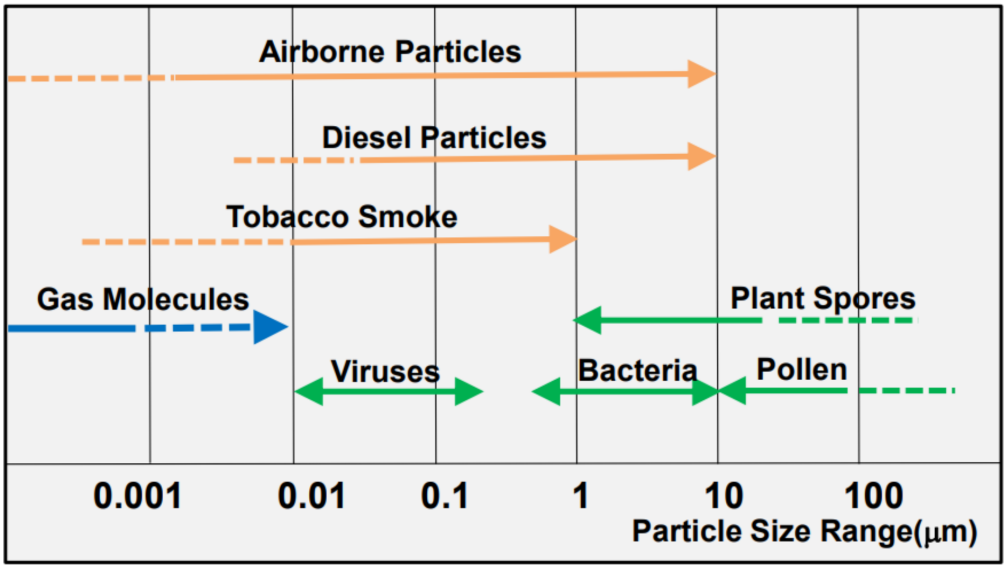

Figure 2.1: Particles size comparison. Adopted from DNV, Aerosol Distribution and Transmission Supported by Ventilation Systems (2021).

Because of these risks, effective control of air pollutants in ship environments requires not only proper ventilation but also advanced filtration and purification technologies capable of removing or inactivating airborne particles across a wide size range. These technologies, their performance, and their integration into marine HVAC systems are discussed in the following section.

2.2 Mechanical filtration system

Mechanical filtration represents one of the most common and effective strategies for removing airborne contaminants in both land based and maritime HVAC systems. Particle filtration can take place in several ways and its mechanics used by the filters can be divided into the following categories: straining, impingement, interception and diffusion. The straining filtration occurs with particles transported by the airflow that have a bigger size of the fiber of the filter media, so the particle is physically too large to pass through and it is therefore trapped on the surface of the filter. However, it is a very ineffective method of filtration because the vast majority of particles are far smaller than the spaces between fibers. In contrast, impingement occurs when large and heavier particles due to their inertia, are not able to follow the curved air streamlines as they curved around the fibers of the filter. As a result, they do not follow the air stream and collide with a fiber. Filters using this method are often coated with an adhesive to help fibers retain the dust particles that impinge on them. Alternatively,, interception occurs when particles following the air flow streamlines come close enough to a filter fiber that they get trapped by it, due to the difference in electrostatic charge. Finally, diffusion mechanism occurs with the smallest particles, as they move with an irregular motion due to the Brownian motion. This random motion causes the contact with the filter fiber, where the particle gets stuck. Diffusion is the primary mechanism used by most extremely efficient filters, such as HEPA filters, which are designed to remove particles well below 1 µm. The different particle filtration mechanisms are shown below in Figure 2.2.

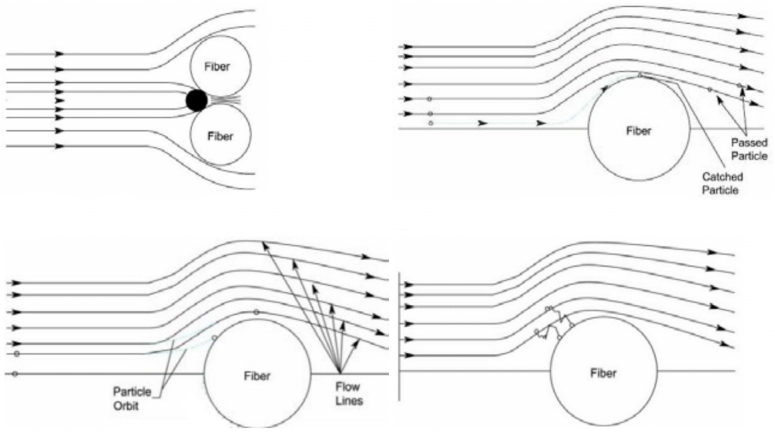

Figure 2.2: Different particle filtrations. Top left: Straining. Top right: Impingement. Bottom left: Interception. Bottom right: Diffusion. Adopted by Heinen and Hopman, white paper (2020).

2.2.1 Air Filter Classification Systems: ISO 16890, MERV and EN 779

Air filters performance has historically been assessed using various standards, each with distinct methodologies and regional applications. The MERV [4] system, enstablished by ASHRAE standard 52.2, is used to evaluate the efficiency of an air filter based on how effective it is at catching particles ranging from 0.3 to 10 µm. The higher the MERV rating, the higher the air filtration capabilities of a particular filter. The lowest level of filtration is 1, and the highest level is 20. MERV is a common system in North America that gives a simple numerical rating, but it doesn't directly relate to the PM [5] classifications. In contrast, the European standard EN 779 classifies filters into groups G1 to F9, referring to particulate air filters for general ventilation. This European Standard is applied to air filters having an initial efficiency of less than 98% taking into consideration 0,4 µm particle sizes. However, EN 779 had limitations in representing real world filter performance across diverse sizes of the different particles. In order to overcome these limitations, the ISO 16890 standard was introduced in 2016, replacing the EN 779 standard. It classifies filters based on their capacity to remove particulate matter in three different size fractions: PM10 ($\leq$ 10 µm), PM2.5 ($\leq$ 2.5 µm) and PM1 ($\leq$ 1 µm). Filters achieving less than 50% efficiency are labelled ISO Coarse, whereas filters with over 50% efficiency are classified as ePM1, ePM2.5 or ePM10.

[4] Minimum Efficiency Reporting Value

[5] Particulate Matter

Type Of Filter	MERV RATING	EN779 Classification	ISO 16890	Particle Size	Common Applications	Available Products
Coarse	MERV 1	G1-G4	ePM Coarse (<50%)	< 20% for particles ≥ 10 microns	Pre-filters	Filter Mats
	MERV 2					
	MERV 3					
	MERV 4					
	MERV 5	G3-G4	ePM 50-70%	20-35% for particles ≥ 3 microns	Residential & Commercial, HVAC Systems, Pre-filters, Spray Booths	Panel Filters, Filter Mats, Spray Booth Filters
	MERV 6					
	MERV 7					
	MERV 8					
Fine	MERV 9	M5-M6 (F5-F6)	ePM10 65%-80%	40-75% for particles ≥ 1 micron	Commercial & Industrial	Pocket Filters, Filter Mats, Spray Booth Filters
	MERV 10					
	MERV 11					
	MERV 12					
	MERV 13	F7	ePM2.5 >65%	75-85% for 0.3-1.0 microns	Residential & Commercial, HVAC Systems	Bag Filters, Rigid Bag Filters, Pocket Filters, Filter Mats, V Cell Filters
	MERV 14	F8-F9	ePM1 70%-80%	85-95% for 0.3-1.0 microns	Environments requiring high air quality (e.g. hospitals)	Bag Filters, Pocket Filters, Filter Mats
	MERV 15					
	MERV 16	F9	ePM1 >80%	95-98% for 0.3-1.0 microns	Critical applications (e.g., cleanrooms, laboratories, operating rooms)	Bag Filters, Rigid Bag Filters, Pocket Filters, Filter Mats

Figure 2.3: Air Filter Efficiency Classification. Adapted from Airguard Envirocare est. (1985).

2.2.2 High Efficiency Particle Filters

High efficiency particulate air (HEPA) filters and ultra-low penetration air (ULPA) filters are designations for specialized filters designed to filter dry air with a rated efficiency of 99.97% or greater. HEPA filters are one of the best ways to filter air mechanically right now for cleaning up recirculated air. HEPA filters were first made for cleanrooms and medical settings, but they are now used in more and more places, including on planes and passenger ships. The filter media is made of glass fiber, which lets them filter out 99.97% for particles of 0.3 µm of size diameter. Moreover, the filter can deal with concentration of PM10 and PM2.5, exhibiting a very high dust holding capacity (DHC). Studies conducted by Shi et al.[6], have shown that glass fiber filters exhibit their lowest filtration efficiency within the particle size range of 0.1 to 0.3 µm, commonly referred to as the most penetrating particle size (MPPS). However, as measured by Guan et al.[7], these filters are able

[6]Shi B, Ekberg LE, Langer S. Intermediate air filters for general ventilation applications: an experimental evaluation of various filtration efficiency expressions.(2013)

[7]Guan J, Jia Y, Wei Z, Tian X. Temporal variations of ultrafine particle concentrations in aircraft cabin: a field study. Build Environ.(2019)

to filter ultrafine particles with 0.1 µm size diameter.

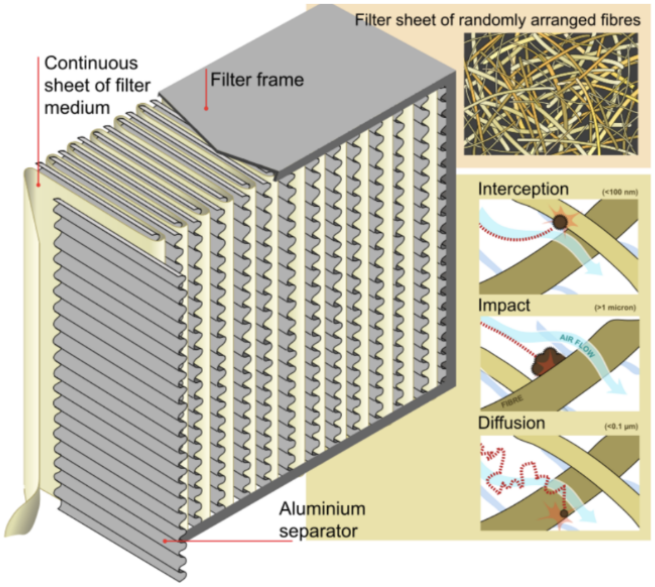

Figure 2.4: Structure of a HEPA filter. Source: Wikipedia (accessed 12 March 2025)

In addition to HEPA filters, the ISO 29463 and EN 1822 standards define two other major classes of high efficiency filters: EPA (Efficient Particulate Air) and ULPA (Ultra-Low Penetration Air) filters. These type of filters differ primarly on their filtration efficiency, with EPA filters representing the lowest filtration efficiency among this classification system, ranging from 85% to 99.5%. Even if EPA filters do not represent an high level of filtration such as the HEPA filters, they are well suited for applications where moderate filtration is sufficient and lower pressure drop is needed, making them a practical option for less critical environments. However, ULPA filters offer a better filtration efficiency, capturing at least 99.9995% of particles with a sized diameter of 0.12 µm. These filters are mainly used in environments where the highest air purity is essential, such as medical or pharmaceutical production, and are barely adopted in passenger vessels. Due to their dense structure to capture small sized particles, they usually generate high pressure drops and require frequent maintenance, increasing the operational costs of the entire system. For these reasons, in maritime environments, where space and energy are constrained, and maintenance access is limited, EPA or HEPA filters offer a more practical and cost balanced solution to maintain safe indoor air quality standards. A study conducted by Heinen and Hopman (White paper, 2020), tested the filtration and penetration efficiency of HEPA filters taking into account the particle size of 0.3 µm. The Figure 2.4 shows the result of the study,

with filters groups being classified according to the standard EN 1822.

Filter group	Class	MPPS integral values		MPPS local values	
		Efficiency (%)	Penetration (%)	Efficiency (%)	Penetration (%)
EPA	E10	85	15	-	-
	E11	95	5	-	-
	E12	99,5	0,5	-	-
HEPA	H13	99,95	0,05	99,75	0,25
	H14	99,995	0,005	99,975	0,025
ULPA	U15	99,9995	0,0005	99,9975	0,0025
	U16	99,99995	0,00005	99,99975	0,00025
	U17	99,999995	0,000005	99,999975	0,000025
MPPS: Most penetration particles					

Figure 2.5: Filter groups. (Adopted from Heinen and Hopman, white paper, 2020)

Even if HEPA and EPA filters can achieve high efficiency standards regarding the filtering methods, is important to take note that the higher the class of the filter, the higher the filter costs and pressure drops within the ducts of the HVAC system, which can lead to higher operational costs. HEPA filters also require more space and maintenance, therefore, they are not always an option.

2.3 UVGI System

Ultraviolet (UV) radiation is a portion of the electromagnetic spectrum with wavelengths shorter than the visible light, raging from 100 to 400 nm (as shown in Figure 2.5). The UV wavelength spectrum can be categorized into three different type of ranges and bands: UV-A (long wave; 315 to 400 nm), UV-B (Medium wave; 280 to 315 nm) and UV-C (short wave; 100 to 280 nm). While UV-A and UV-B wavelengths are transmitted by the sun and are responsible for skin aging and sunburn, the UV-C wavelengths are absorbed by the ozone layer and does not reach the Earth's surface. For this reason, UV-C lights are artificially produced by germicidal UV sources such as lamps. As reported by the ASHRAE Handbook (HVAC and Equipment, 2024), the most effective UV wavelength range for inactivation of microorganisms is between 220 and 300 nm, with maximum effectiveness near 265 nm. However, most commercially UV-C lamps reach their maximum relative germicidal efficiency at 253.7 nm. Ultraviolet germicidal irradiation (UVGI) systems operating in the UV-C spectrum have been largely used in air ducts, air handling units, upper rooms, and portable disinfection devices and their adoption is becoming increasingly frequent as awareness grows regarding energy efficiency,

maintenance needs, and indoor air quality conditions. In the Figure 2.5 below, it is shown the Ultraviolet light spectrum and classification.

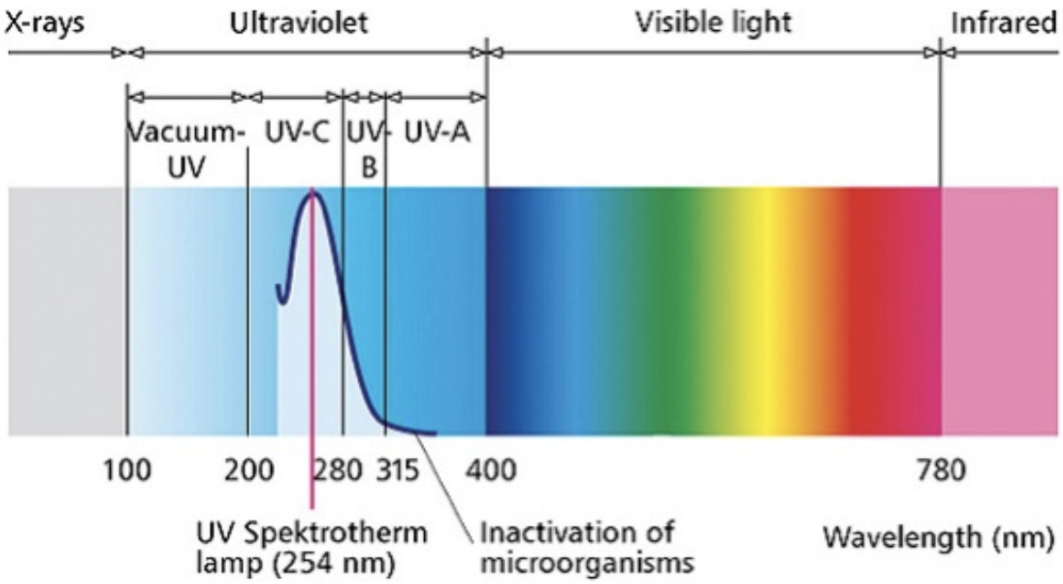

Figure 2.6: Ultraviolet light spectrum. Source: Wikipedia (accessed 12 March 2025).

2.3.1 Effectiveness of the System

The UV energy inactivates microorganisms by damaging their DNA and RNA structure, not allowing them to reproduce anymore. The effectiveness of the UV-C system in air disinfection depends on several factors, such as the dose of the UV-C light used, the type of microorganisms and the light positioning. The dose $[mJ/cm^2]$ is described as the irradiance[8] $[\mu W/cm^2]$ received at the target area multiplied by the exposure time[9] $[s]$.

$$\text{Dose } [\text{mJ/cm}^2] = \frac{\text{Irradiance } [\mu\text{W/cm}^2] \times \text{Exposure Time [s]}}{1000} \tag{2.1}$$

The required dose varies depending on the different pathogen to be neutralized. Viruses and bacteria are the most susceptible to UV-C radiation, thus they require lower doses for inactivation, while mycobacteria, bacterial spores, and fungal

[8]Irradiance is the amount of electromagnetic radiation energy striking a surface per unit area, commonly expressed in microwatts per square centimeter ($\mu W/cm^2$).

[9]Exposure time is the time that a surface or microorganism is exposed to the UV radiation.

spores are the most resistant and they usually need an higher level of UV-C dose. Additionally, other factors, such as temperature, humidity, air velocity, physical parameters of the duct and duct reflectance can influence the UVGI system performance. High relative humidity, for instance, can reduce the effectiveness of the UV-C radiation by increasing light scattering and absorption by water molecules, leading to a decrease in the amount of UV light that reaches the pathogens targeted for inactivation. Moreover, UV-C light can be used to sterilized the air from airborne microorganism or as surface disinfection to inhibit the growth of mold and bacteria in specific areas. Consequently, the optimal placement of the UV-C sources depends on the application and the location where the microbial control is most needed. For air disinfection, airflow must pass through a well irradiated region within the duct system, where light reaches further and longer exposure time and UV lamps are positioned to minimized shadowed areas and ensure constant exposure. However, the number of lights increases the air temperature, therefore, according to the white paper published by Heinen & Hopman (2020), the best location to place the lamps is in front of the cooling block perpendicular to the airflow, providing both surface disinfection for the cooling block[10] and air disinfection. In surface disinfection, the static positioning of the component allows the target area to be exposed to UV radiation for a continuous exposure time, making the microbial growth easier to control.

2.3.2 Low Pressure Mercury Vapor Lamps

Among the various technologies used to generate UV-C radiation for air and surface disinfection, low pressure mercury vapor lamps and UV-C light emitting diodes (LEDs) represent the most common solutions currently used in HVAC systems. In this section, we will look at these two different technologies to see what their pros and cons are in terms of efficiency, operational performance, and environmental impact. According to ASHRAE (Handbook 2024), low-pressure mercury discharge lamps are the most energy-efficient UV-C lamps and the ones that people use the most. These lamps contain mercury, which evaporates when the lamp is switch on. The electric field in the discharged tube makes mercury atoms move faster and hit noble gas atoms. This makes the mercury excited and emit ultraviolet radiation. The excited atoms emit around 85% of their energy at 253.7 nm wavelength, reaching their maximum UV output when the cold-spot[11] temperature of the lamp is between 38 and 50°. The UV output value is linked to the vapor pressure inside the lamp, which reaches its optimal value under still air conditions at 25°. In

[10]Contamination on the cooling coil can increase the pressure drop and reduce airflow and heat exchange efficiency.

[11]Coldest portion of the UV lamp during lamp operation.

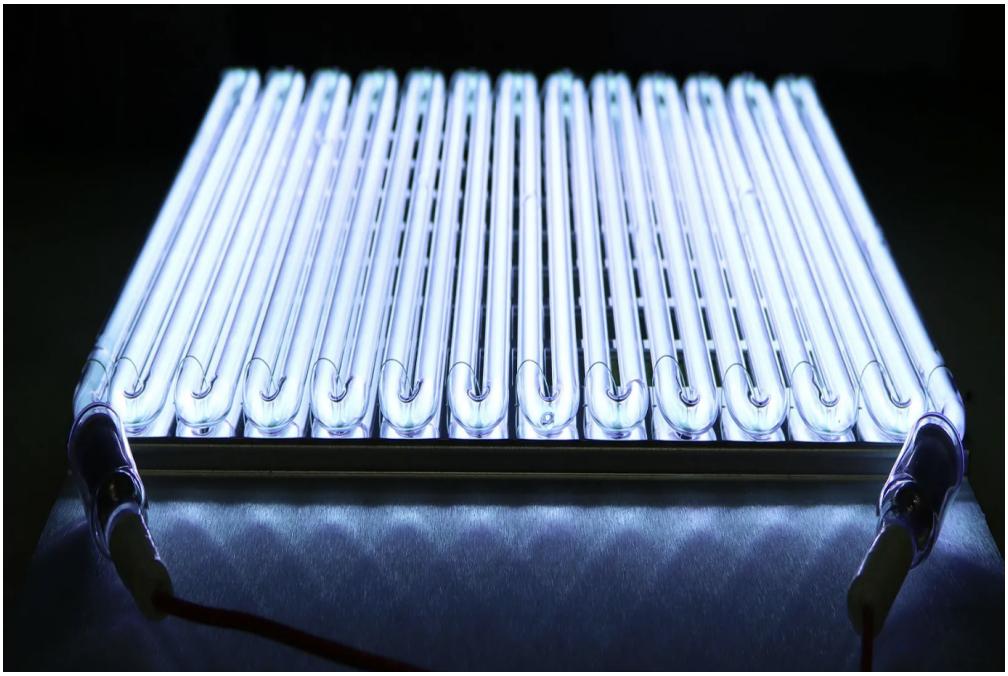

Figure 2.7: Low Pressure Mercury Lamps. Source: Jelight Company Inc. Official website. Available at: https://www.jelight.com/low-pressure-mercury-lamps/ (accessed 6 April 2025).

moving air, the cold-spot temperature may be too low to reach an optimal UV output, therefore, special windchill-corrected lamps can be used to overcome this problem. According to the ASHRAE (Handbook, 2024), Figure 2.6 shows how lamp output varies as a function of the cold-spot temperature.

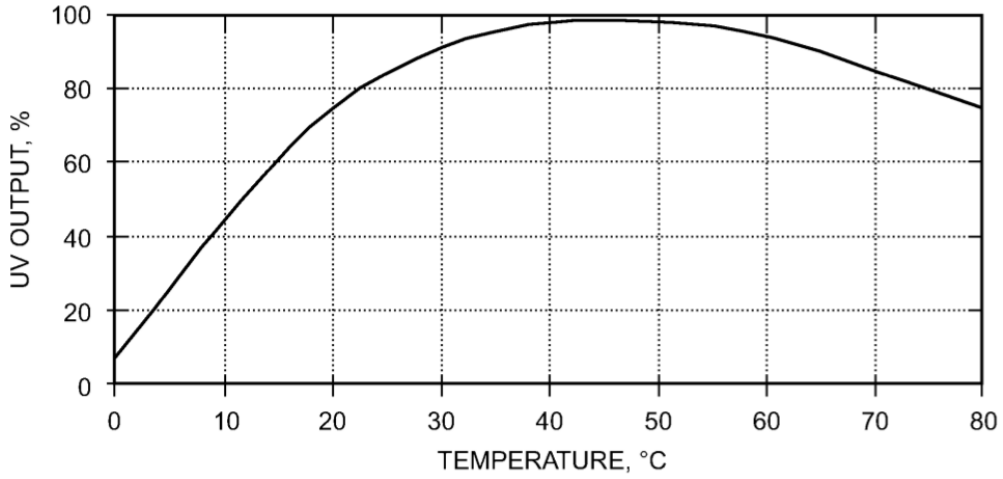

Figure 2.8: Low Pressure Mercury Lamp Output as Function of Cold-Spot Temperature. Source: ASHRAE Handbook – HVAC Systems and Equipment, 2024.

Despite their common use in air handling unit applications, mercury based UV-C lamps present some limitations. They have mercury in them, which is a poisonous substance that can hurt the environment and people's health. They also need to warm up to full intensity, and they tend to make heat while they work, which can affect the HVAC system's overall thermal balance.

2.3.3 UV-C LEDS

In recent years, UV-C LED technology has been adopted into HVAC equipment for several germicidal applications, becoming a promising alternative to low pressure mercury lamps.

LEDs are solid state devices designed to emit the maximum wavelengths emissions in the range that goes from 260 to 280 nm, when used for germicidal applications. In contrast with the previously described mercury based lamps, their ability to operate immediately, since they do not require a warm-up time to stabilize the output, and the absence of mercury, make the UV-C LED a better alternative from both environmental and practical standpoint. UV-C LEDs are made of semiconductor materials deposited on substrates, which emit directional ultraviolet radiation through direct bandgap electronic transitions. The circuit board components can run both in series, parallel and mixed circuits, making them a more flexible solution for system integration, also due to their compact size directional emission. LED technology is also well known to its low enrgy consumption, offering a clear energy saving advantage with respect to the mercury based lamps. However, Their UV

Figure 2.9: UV-C Led lamps. Adopted from Halton Oy study material.

output is significantly lower compared to mercury lamps, which can require longer exposure times or the UV-C LED to be placed in proximity of the target to be disinfected. Moreover, humidity, risk of condensation and circuit temperature must be carefully taken into consideration to guarantee the optimal performance of the system. However, the spectral output of UV-C LEDs designed for germicidal applications is typically engineered to avoid emissions below approximately 242 nm, the threshold at which ozone generation begins. As a result, germicidal UV-C LEDs generally do not produce ozone.

2.3.4 UV Photocatalytic Oxidation

In addition to the technologies described above, recent technological developments have introduced systems that inactivate indoor air pathogens by using the photocatalytic oxidation technology. A study conducted by Teresa M. Mata et Al. (2025), illustrates how these systems, known as UV-Photocatalytic Oxidation (UV-PCO), by the combination of ultraviolet light and a photocatalytic surfaces, typically made of Titanium dioxide T_iO_2, generate higly reactive oxygen species (ROS) that remain surface bound when exposes to UV-A or UV-C light. These species are

higly reactive with organic and biological pollutants present in the air, breaking their molecular structure and turning them into non dangerous byproducts such as carbon dioxide and water. Moreover, unlike ozone based oxidation technologies, UV-PCO systems do not generate ozone, making them a safer alternative for living and occupied spaces. The air needs to move over the photocatalytic surface, where the reactive oxiders are made and work on pollutants almost right away. The process can also get rid of volatile organic compounds (VOCs), odors, and aerosolized chemical pollutants, in addition to viruses and bacteria. But the system's effectiveness depends on a number of things, such as the UV wavelengths and intensity, the humidity levels, and the way air flows. If oxidation isn't done completely, byproducts like formaldehyde or acetaldehyde could be made, which could be bad for people. To mitigate these issues, we need to think about using both PCO and filters to cut down on the amount of these byproducts in the environment. On the other hand, even if the PCO is a complex system to design, due to its dependency on a wide range of factors such as environmental and design designations, it has several advantages due to its low energy consumption of heterogeneous photocatalytic oxidation, low pressure drops, long life cycles of reactive process and the use of solar light.

2.3.5 Maintenance and Safety Precautions

The implementation of the UVGI technologies requires consistent and well planed maintenance to ensure good performances of the system. UV lamps should be replaced at the end of their useful life. For low pressure mercury UV-C lamps that have a continuous operation, the useful life time should be around 9000 h, but this value could change depending on the design operations or manufacturer recommendations. Moreover, turning lights on and off may decrease their useful life, leading to an early failure of the lamps. For these reasons, changing lamps annually may be a good choice in order to keep the optimal operation of the UVGI system. On the other hand, LED UV-C lights are typically not affected by frequent on and off power switching, but they require regular cleaning of quartz windows in order to maintain good level of UV-C radiation emitted. Furthermore, unlike the low pressure mercury lamps, the UV-C LEDs maintain their germicidal output for longer periods of time, wiht a useful life raging from 10,000 to 25,000 hours, depending on thermal condition, chosen drive current and environmental conditions. In addition to regular maintenance, the implementation of UVGI systems must account for safety precautions aimed at protecting both equipment and occupants. UV-C radiation is invisible to human and might be harmful to human tissue, causing skin erythema and ocular damage under a direct exposure of the radiation. Another important part is the production of ozone, which happens when UV-C lamps emit wavelengths shorter than about 240 nm. Ozone is a poisonous gas that

can be harmful when inhaled, causing respiratory irritation and other health risks. For this reason, most germicidal UV-C systems made for use in occupied spaces are made to avoid making ozone by sending out wavelengths around 253.7 nm.

2.4 Ionization Based Air Purification Technology

Ionization based air purification is a technology that introduces ions, generally negative, into the space to purify. The ions are produced by exposing the air molecules to a very high voltage, which causes them to lose or gain an electrons, thereby creating charged particles. These ions then attach to allergens and pollutants in the air, like dust, viruses, volatile organic compounds, and bacteria, to cancel out their electrostatic charge. The ionizer makes these particles bigger and heavier, which makes them fall to the ground instead of staying in the air. Some of the harmful pollutants are taken out of the air this way, which lowers the chance of breathing them in. As reported by a study conducted by Pushpawela et al. (2017), ionization systems showed good performances on reducing airborne pollutants in indoor environments. In their study, a small negative ion generator installed in a closed test chamber was able to remove up to 70% of airborne particles within 15 minutes. Furthermore, when tested in ventilated rooms, the overall particle reduction of the ionizer outperformed the one of the HEPA filters, thanks to the ability to spread ions through the HVAC ducts.

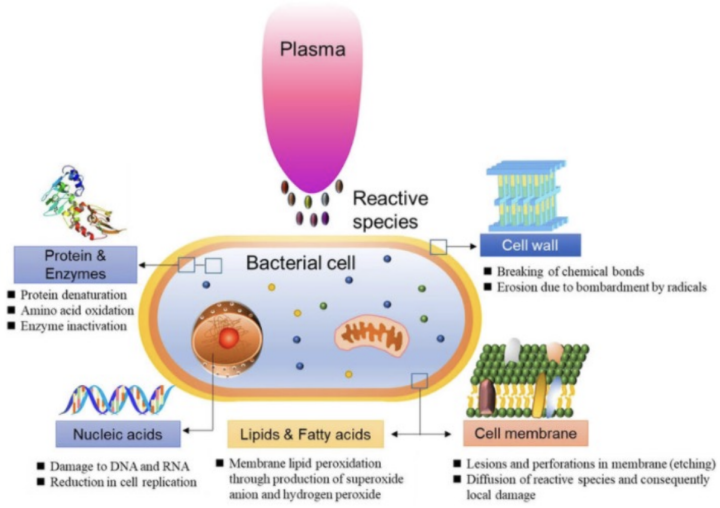

Figure 2.10: Ionization process. Adopted from AirForte Oy study material.

This evidence shows how ionization systems could be particularly effective in applications that require low pressure drops, since their technology do not rely on

physical filters. However, there are few limitations associated with this technology that must be considered. Ionization efficiency also decreases with distance from the ion source, making them a less effective solution in spaces with limited airflow. They also present a lower efficiency with respect to HEPA filters when adopted in smaller rooms. Ionizers can also make ozone and other oxidized molecules, which can be harmful to people if they aren't kept in check. Another important thing is maintenance. Even though the filters don't need to be changed, the electrodes and other parts need to be checked and cleaned often to keep working well over time, which costs more to run. However, the ionization based technology are usually integrated into HVAC systems as a complementary system rather than a standalone solution. They are particularly effective when combined with a mechanical filtration apparatus or with UV based disinfection solution, leading to a more efficient air cleaning system, especially in crowded and high volume ventilation contexts like passenger ships.

Chapter 3

Case Study: Passenger Vessel

3.1 Ship Overview

3.1.1 General Description

Figure 3.1: Example of a modern passenger vessel, representative of the type of ships considered in this study. Adopted from Quality travel's website. Available at: https://www.qualitytravel.it/grandi-navi-veloci-festeggia-unestate-da-record-ai-gnv-awards/115367 (accessed 10 April 2025).

The passenger vessel that we are considering for our study, is a cruise ferry that mainly runs between Helsinki and Stockholm. The ship is about 203 meters long, 31.5 meters wide, and has a draft of 7 meters. Its gross tonnage is about 58376 GT. The ship can reach about 21 knots and it is powered by four Wärtsilä-Vasa 9R46 diesel engines that together produce about 32,580 kW. The ship has a total of 13 decks, of which 12 are accessible to passengers and crew and can carry up to 2800 passengers with parking spaces for around 450 cars. Moreover, There are also more than 900 passenger cabins on different decks, each with a different layout to fit the needs of different types of travelers. The most space- and cost effective option is a standard inside cabin, which is located in the middle of the ship and can hold 2 to 4 people. Because they are on the inside of the ship and don't have access to natural light and air flow, they depend entirely on the mechanical filtration system to keep the air clean and comfortable. Standard seaside cabins, on the other hand, do have windows or portholes that let in natural light and provide a view of the sea. Cabins with promenade views are on decks 8-11 and face the ship's central atrium. They have large windows that connect them to the main public promenade, giving the impression of a semi-open space. These cabins are located in the middle of the boat, so they don't have a view of the sea or natural ventilation. However, they do have a unique architectural design that makes the experience on board better.

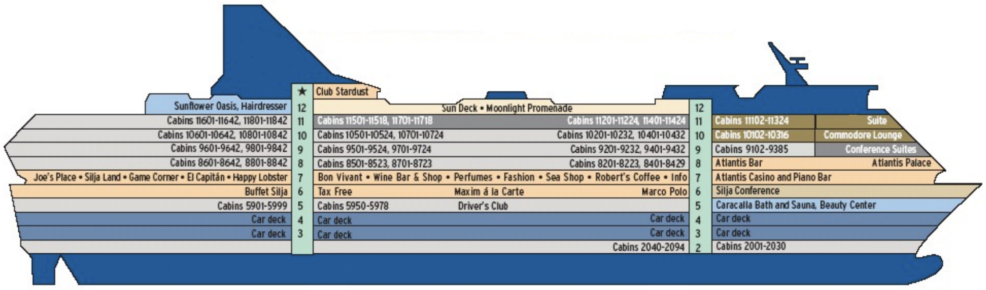

Figure 3.2: Reference passenger vessel deck's plan. Adapted from NaParome website. Avaiable at: https://symphony-silja.narod.ru/.(accessed 10 April 2025).

In addition to these standard categories, the vessel offers a number of upgraded cabin classes intended to provide better comfort and privacy. Family cabins, typically located on decks 8-11, are larger and fitted to guest up to six individuals, making them ideal for groups or travellers with children. Deluxe cabins are located on deck 11th and have more spacious interiors, better furnishings, and often include better sound insulation. Commodore cabins, placed on decks 10th and 11th, are more private and comfortable, usually with access to privileged lounge services. At the high end, suites and executive suites are found on the highest passenger decks,

with increased floor space, panoramic windows or balconies. Their location in less frequented, upper parts of the ship helps provide a quieter atmosphere and better thermal comfort. In addition, the ship offers numerous public space areas such as restaurants, bars, duty-free shops, a spa and wellness complex, entertainment venues.

3.1.2 Capacity and Operational Profile

The ship's operational profile is tailored to operate to short sea routes in the Baltic sea, with a daily service connecting Helsinki to Stockholm, including an intermediate stop in Mariehamn (Åland Islands) in order to meet the duty free requirements between Finland and Sweden. For the reference passenger vessel, the journey from Helsinki to Stockholm typically last 17 hours, depending on weather and traffic conditions, with scheduled departures at 17:00 from the Olympia terminal of Helsinki and arrival the next morning around 10:00 at the Värtahamnen terminal of Stockholm, offering full night passage service. During all the duration of the trip, a continuous HVAC operation is required to ensure thermal comfort and air quality throughout all public and private spaces, particularly during peak occupancy periods. The ship runs throughout the year with peak capacity during summer and holidays season, when tourist demand increases. Consequently, the HVAC system is expected to respond dynamically to changing internal heat gains, humidity loads, and air quality demands according to occupancy and external climatic conditions.

Figure 3.3: All ferry routes operated by Tallink Silja Line between Finland, Sweden, Estonia, Latvia, and the Åland Islands. Adopted from Tallink Group official website. Avaiable at: https://www.tallink.com/ (accessed 11 April 2025
.

The ship's crew is composed of approximately 264 members, including hotel, technical, and navigation staff, who are provided with separate accommodation

in areas reserved for crew members only. This operational framework, which has a lot of passengers coming and going, continuous service, and changes in the seasons, generates significant demands on the ship's environmental control systems. Thus, the HVAC system must guarantee reliable, adaptable, and energy efficient performance under a wide range of occupancy and climatic conditions.

3.1.3 Ship's HVAC System Overview

As a large ferry operating mainly overnight voyages in the Baltic sea, the reference passenger vessel must require a centralized HVAC system composed of multiple air handling units (AHUs), fan coil units (FCUs), exhaust fans, and ducts that supply, recirculate, and exhaust air in public and technical areas spread over the ship's decks. The Heating, Ventilation, and Air Conditioning (HVAC) system mainly relies on AHUs that treat the air and supply it to different zones. The units are usually located in technical spaces and supply several cabins or public areas through a large network of insulated ductworks. Fan Coil Units are used to control the temperature of the air in passenger areas like cabins, restaurants, lounges, and recreational areas. They get their supply air from central units and their return air from ceiling or wall intakes. According to the maritime air quality standards (e.g., ISO 7547:2022), the ventilation system operates in partial ventilation mode, which usually consist of approximately 30% of fresh air intake and 70% of recirculated air. This configuration is designed to achieve better energy efficiency, particularly in colder winter environments. Fresh air intake is filtered, conditioned, and blended with recirculated air before being distributed to the indoor areas of the ship, while galleys, laundries, toilets, and engine rooms, must operate on 100% fresh air supply and exhaust, since these areas are characterized by high air change rates and minimal cross contamination risks.

3.2 Selected Test Area: Sunflower Oasis

The study of this thesis will be focused on a single well defined ventilation zone of the ship: the Sunflower Pool Area, which is ventilated by the Air Conditioning Unit AC 232 located in AC room 25. This space is located on Deck 12 of the reference passenger vessel and it's part of the ship's onboard Spa and wellness complex called Sunflower Oasis. It is a recreational space for passengers and includes three heated pools, whirpools, seating zones, a pool bar where it is possible to order drinks and snacks, and a large surrounding windows offering external views. Moreover, the Sunflower Oasis is equipped with separate saunas for men and women, a communal steam sauna, a private sauna and also a kids' pool with a slide for families with children. Due to its intended use and architectural layout, the Sunflower Pool Area represents a particularly challenging environment from a

ventilation and air quality perspective. The space is characterized by high relative humidity and elevated ambient temperatures, typically ranges between $30 - 32°C$ to ensure thermal comfort for bathers, since the temperature at the pools is set to maintain $36°C$.

Figure 3.4: Sunflower Oasis Pool Area. Adopted from Tallink Group official website. Avaiable at: https://www.tallink.com/on-board/spas-saunas (accessed 11 April 2025

.

The relative humidity levels in the zone are much higher than in other parts of the vessel, usually between 55% and 65%. This is because of the presence of warm water surfaces, always present, human occupancy, and reduced natural air exchange. These environmental conditions make this area ideal for testing air purification performance, especially under conditions favorable to microbial and fungal proliferation if ventilation is inadequate. According to the HVAC ducting layout, the Sunflower pool area has several supply and exhaust terminals distributed throughout the three water pools: a central main pool and two lateral whirlpools. This system of supply and exhaust grilles is designed to ensure adequate air exchange, and maintain thermal comfort in a space characterized by warm water surfaces and continuous occupancy.

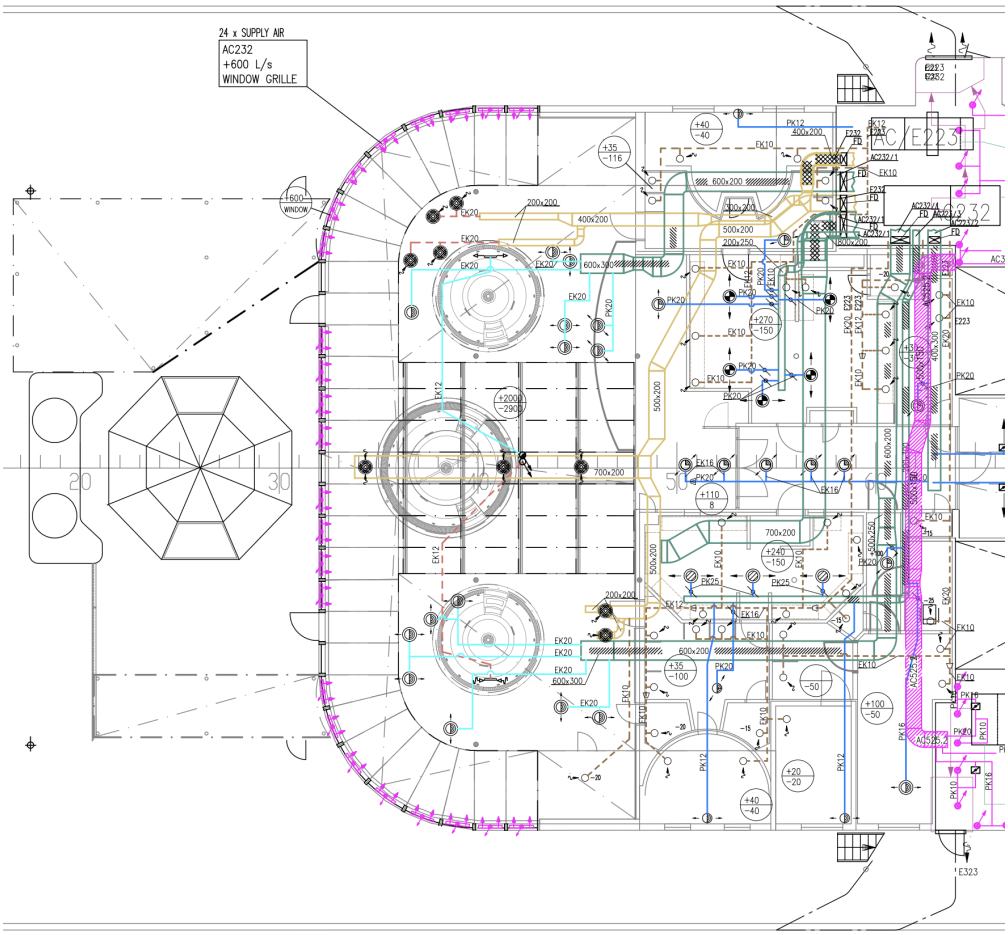

Figure 3.5: Technical ventilation layout of the Sunflower Pool Area (AC232), located on Deck 12 of the reference passenger vessel. The figure shows where the supply air grilles and exhaust air grilles are located. There are specific extraction points near the three main pools to control humidity and make sure the air is always fresh. Image adapted from the vessel's HVAC documentation.

In total, 9 exhaust air grills have been installed in the Sunflower Pool Area, represented as a black gridded circle as shown in Figure 3.5 that illustrates the ventilation plan. These terminals are designed to extract humid and warm air saturated with water vapor from the proximity of the pool surfaces. In addition to the exhaust grilles, there are a total number of 14 supply air terminals, represented as a geometric icon featuring layered concentric outlines crossed by a vertical line, distinguishing it from the exhaust outlets. These terminals, installed on the ceiling perimeter of the spa zone, supply a constant, filtered, and conditioned air flow at a controlled temperature and velocity, helping to control temperature stratification

and avoid stagnant, humid areas. As we can see from Figure 3.5, the central pool is equipped with 3 exhaust grilles arranged along its perimeter in order to capture rising moist air and reduce the risk of condensation. On the left side whirlpool (as viewed when entering the area) there are 7 supply air terminals and 2 exhaust air grilles located near the edge of the water, while on the right side whirlpool there are 7 supply air grilles and 4 exhaust air grilles installed on the ceiling around the pool's perimeter. Each supply point is connected to the centralized HVAC system and designed to deliver conditioned air at a controlled temperature and flow rate. Looking at the pipes configuration, the ventilation system is connected to the ship's ducting through rectangular and round sections and relies on two separate duct networks clearly distinguishable in the technical drawings by two different colors. The supply air ducts, represented in cyan, have a dimension of 600 x 200 mm, with a rectangular cross section and are connected to ceiling mounted diffusers for supply air. On the other hand, the exhaust air ducts, represented in yellow, varies in cross-sectional size based on its position in the Sunflower Pool Area. From the air handling unit AC232, the first exhaust duct is 500×200 mm, expanding to 700×200 mm in the middle pool area to accomodate greater airflow requirement. Within the right whirlpool zone, the duct steps down to 400×200 mm, and further reduces to 200×200 mm at the extraction terminals. On the left-hand side of the area, the exhaust branch also has a 200×200 mm duct directly to the grilles. This stepped reduction is a zoned extraction approach, aimed at maximizing airflow efficiency and ensuring uniform ventilation performance throughout the spa space.

Lastly, the configuration of the supply and exhaust units ensures a balanced ventilation system, with localized extraction near the pools and general diffusion in surrounding areas. This keeps the indoor air quality and temperature in line with the design standards needed for wellness centers.

Figure 3.6: Left-side whirlpool

Figure 3.7: Right-side whirlpool

3.2.1 Current HVAC system: AC232

The HVAC system serving the Sunflower Pool Area (Zone AC232) is a central air handling system in AC Room 25, designed to supply and extract air in the spa area on Deck 12. The air handling unit AC232 is made of a complete set of functional elements for air filtration, thermal treatment, humidity control, and regulation of ventilation flow. It operates in automatic mode, adapting the system based on the seasonal changeover between summer and winter operation. For the purposes of this study, only the summer condition case will be taken into consideration.

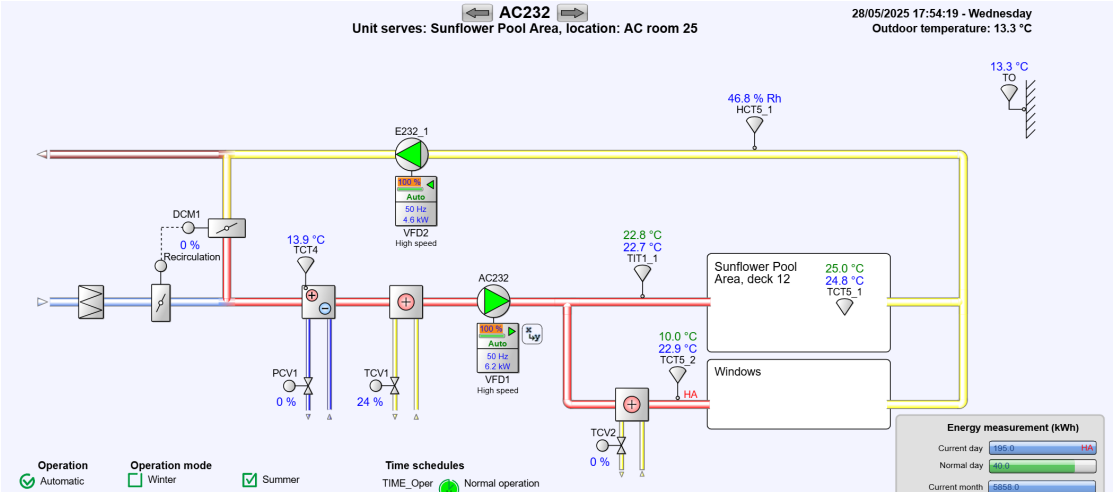

Figure 3.8: HVAC system AC232 serving the Sunflower Pool Area on Deck 12.

As shown in Figure 3.8, the system is divided into two primary branches: the supply air line and the exhaust air line, each provided with separate fans, valves, and temperature/pressure control devices. On the supply side, the air that comes into the system goes through a F7 filter, which is a medium to high efficiency filter that can get rid of at least 65% of particles in the $0.3 - 1$ μm range, according to the ISO 16890 standard. These filters are often used in HVAC systems to keep the air inside clean by getting rid of small particles like dust, pollen, and germs. The fresh air goes into a mixing area after it has been filtered. This area is controlled by a Damper Control Module (DCM). This module moves a mixing damper to change how much recirculated air is in the system. This device allows a portion of the extracted air to re-enter the supply line, where it is mixed with the filtrated fresh air before moving forward to the different stages of the HVAC system. The recirculated ratio is set to 0% in the current setup (see Figure 3.8). This means that only fresh air is being sent to the system. However, this number could change based on the operational conditions, the outside temperature, the humidity, and the number of people present in the room. Typically, under operational conditions,

the HVAC systems are designed to maintain a ratio of 70% fresh air and 30% of recirculated air, ensuring both energy efficiency and good air quality levels. During the current summer operating conditions, the HVAC system AC232 runs without turning on the preheating coil or the humidifier because the main goal is to lower the temperature and humidity of the outdoor air before it is sent to the Sunflower Pool Area. Thus, the air passes through the preheating coil unit, which is bypassed due to the summer operational mode configuration, as indicated by the the water valve (PCV) being fully closed (0%). This means that there is no circulating hot water through the coil, and its role as a thermal buffer or frost protection (only employed in winter mode) is switched off. The air passes through this part without any notable temperature change, where a Temperature Control Valve (TCT4) checks its temperature, which is $13.9°C$, while the outdoor temperature is $13.3°C$, as displayed by the TO valve. The air then passes to the cooling coil unit, which is not specifically labeled as a separate box but functionally is placed directly downstream of the bypassed preheater. Here, the air is actually cooled by chilled water, lowering both its temperature and absolute humidity. After the cooling period, the air goes through a unit called a Post Heating Coil, which is also known as a Reheating Coil. The TCV1 valve controls this part, and it is currently open at 24%, which lets hot water flow through. The purpose of this coil is to raise the temperature of the air after dehumidification, thus providing thermal comfort to the occupants and avoiding the sensation of cold drafts. Subsequently, the conditioned air is transferred to the distribution system through the supply fan AC232, which operates at its full load (100%, 50 Hz, 6.2 kW). Finally, the duct system splits into two separate branches: one of which directs conditioned air straight to the Sunflower Pool Area, while the other is reserved exclusively for winter months to prevent condensation on the windows of the room by supplying warm air along the glazing surfaces. This secondary duct can be bypassed during summer, as it carries no functional significance when outside temperatures are higher and condensation is not a problem. On the Sunflwer pool duct side, a Control Valve Temperature TIT1_1 displays the air's set point temperature (the one showed in green color) and the actual air's temperature (the one shown in blue color), which are respectively $22.8°C$ and $22.7°C$.

Lastily, the airflow is then supplied to the spa area through dedicated ducts and diffusers, such as ceiling mounted grilles and window integrated terminals, providing consistent comfort conditions throughout the zone where another Temperature Control Valve (TCT5_1) checks the actual temperature of the air being $24.8°C$.

On the exhaust side of the AC232 HVAC system, air handling starts with the pickup of return air from the Sunflower Pool Area. This air is generally warm and moisture laden as a result of the heated water surfaces and high occupancy. The exhausted air is routed through a dedicated exhaust duct, which directs it to either recirculation or final expulsion outside the vessel.A Humidity Control

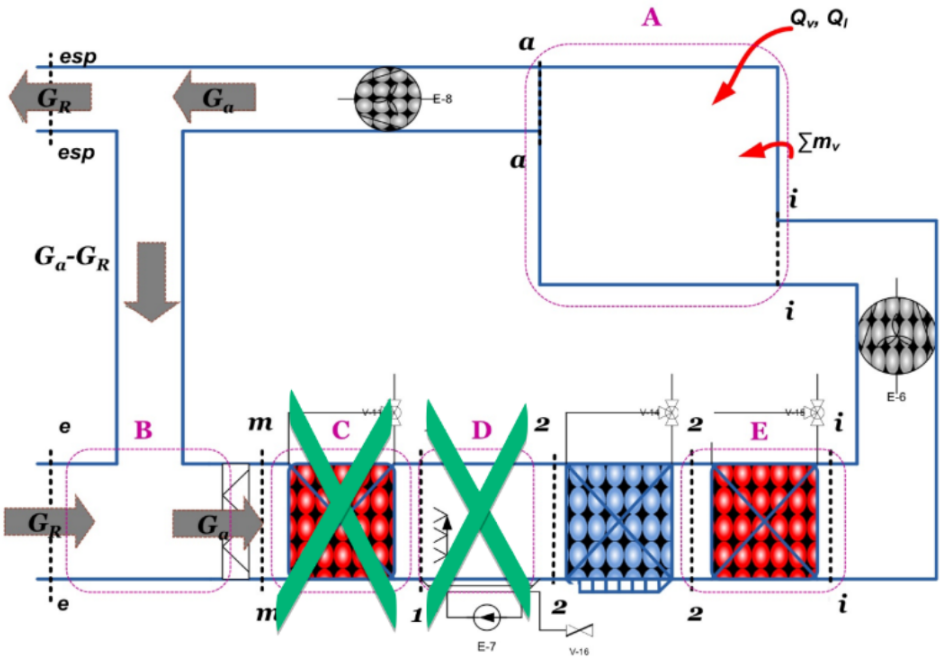

Figure 3.9: Standard HVAC summer case configuration with control volumes C and D (Pre-heater and Humidifiyer) being bypassed due to the summer case operational mode.

sensor (HCT5_1) checks the air's relative humidity as it moves toward the exhaust line. This sensor shows that the relative humidity is 46.8% under the current summer conditions, which shows that dehumidification works during the supply stage. Moving forward to the system, the air is pushed through the exhaust fan (E232_1), which operates at full capacity (100%, 50 Hz, 4.6 kW), ensuring the continuous removal of saturated air from the conditioned space. This fan creates the necessary pressure to drive the exhaust flow through the ducting and towards its destination. After the fan, The duct then divides into two branches to create a diverging exhaust line: One path goes directly to the external discharge, where the air extracted is delivered to the outside environment. The next branch enters the recirculation loop, rejoining the mixing section of the supply line via a damper (DCM1). This recirculated air can be mixed back into the system to optimize air quality and energy efficiency.

Chapter 4

Theoretical Case Study Calculations

4.1 Introduction

4.1.1 Purpose and Scope of the Study

The purpose of this chapter is to describe and analyze the performance characteristics of two purely theoretical air purification scenarios, each based exclusively on a single technology:

1. A **mechanical filtration system** using an HEPA filter;

2. An **Ultraviolet Germicidal Irradiation system** (UVGI).

Both systems are regarded as independent configurations, engineered and sized according to identical environmental and operational criteria. The calculations done in this chapter are not meant to suggest real design solutions for immediate implementation. Instead, they are meant to give quantitative reference benchmarks. These benchmarks will subsequently be compared, in Chapter 5, with the real case performance data of the AirForte Aero Quattro technology, in order to assess the relative advantages and demonstrate the potential added value of the Airforte solution in maritime HVAC applications.

The scope of this theoretical analysis is thus intentionally confined to estimating performance metrics directly comparable across the three cases (HEPA, UVGI, Airforte Aero Quattro technology). Specifically, the research will be focus on:

- Improvement in indoor air quality (IAQ) achieved by the system;

- Physical space required for the installation and integration of the air purification unit within the duct network infrastructure.
- Time needed to clean the entire room and reach the desired target air quality level;
- Additional airflow or ventilation capacity required to compensate for the pressure loss introduced by HEPA filtration and maintain the designed air change rate (only for the HEPA filter case);
- Needed UVGI radiation to achieve Log3 (or 99,9%)elimination effect of microbes (only for the UVGI system case);
- Maintenance requirements.

For the HEPA filter case, we will take into consideration the H14 filter class, which according to the EN 1822 and ISO 29463 standards, it is capable of removing at least 99.995% of airborne particles with a diameter $\geq 0.3\mu m$. The analysis examines how this filter would affect airflow in the duct, computes the resulting pressure drop, and estimates the fan power or extra ventilation capacity needed to achieve the desired air change rate. The concept of Clean Air Delivery Rate (CADR) will be used to estimate the IAQ improvement achievable over time, based on the volume of the target space and the operating airflows.

The study will concentrate on microbial inactivation through exposure to UV-C radiation within the germicidal wavelength spectrum, typically at 254 nm. The study will examine the dose-response relationship for airborne microorganisms, determining the dose necessary to attain a Log3 (or 99.9%) reduction of pathogens using the formula $D = I \cdot t$. T This involves selecting appropriate inactivation rate constants (k) for typical airborne pathogens, determining the necessary lamp power and duct placement. We will also take into account space limitations, shielding needs, and possible side effects such as ozone generation or photolytic by-product formation.

By taking a controlled and standardised set of assumptions, the two theoretical cases will provide a neutral performance baseline. This will allow for a direct and meaningful comparison with the Airforte Aero Quattro system, the effectiveness of which has been proven experimentally under real operating conditions on cruise ships. This comparison will serve not only to identify differences in efficiency, but also differences in operational viability, integration complexity, and long-term maintainability. Conclusively, the calculations presented in this chapter do not attempt to design HEPA or UVGI systems specifically for use in maritime environments, but a scientifically structured method to quantify and compare

their theoretical effectiveness with that of a new, multi technology solution. This approach ensures that the conclusions presented in the next chapter are predicated on a clear, consistent, methodical, and evidence based framework.

4.1.2 Characteristics and Operational Parameters of the Theoretical Case Study

In order to perform a methodical and realistic theoretical evaluation of the selected air purification technologies, it is essential to define the basic properties of the ventilation system into which these technologies are going to be applied. The main geometrical, aerodynamic, and operational parameters of the reference duct network are described in this subsection and will serve as the basis for all the calculations presented in this chapter. By defining these parameters, it is guaranteed that the performance comparison between different purification solutions is done under the same operating conditions, thus separating the impact of the technology itself from any potential differences in the ventilation infrastructure.

The duct section under consideration has a rectangular cross section of 450 mm by 250 mm, which has a total area of

$$A = a \cdot b = 0.450 \cdot 0.250 = 0.1125m^2 \tag{4.1}$$

being a and b the side lengths of the duct. For the purpose of aerodynamic analysis, the hydraulic diameter is calculated using the relation

$$D_h = \frac{2ab}{a+b} = 0.321m \tag{4.2}$$

Substituting the given dimensions we can estimate an hydraulic diameter of 0.321 m, corresponding to an effective cross sectional area of

$$A_h = \frac{\pi \cdot D_h^2}{4} = 0.081m^2 \tag{4.3}$$

when considering the internal flow section used in the velocity calculation. This geometrical requirement is critical for determining the regime of flow, calculating Reynolds numbers, and estimating pressure losses through any purification system implemented. The reference airflow rate for the duct is set at 780 L/s, equivalent to 2808 m^3/h. Combining this value with the effective cross sectional area, we can evaluate the air velocity within the duct as follows:

$$V_{air} = \frac{\dot{Q}}{A_h} = \frac{2808}{0.081} \cdot \frac{1}{3600} = 9.63m/s \tag{4.4}$$

which is within the range of typical values found in supply and return ducts of medium capacity HVAC systems. Furthermore, the available pressure before any

filtering system is 900 Pa, representing the upper end of the pressure budget prior to a drastic reduction in airflow occurring.

The room served by these two different theoretical methods has a volume of 460 m^3. At the given airflow rate, we could calculate the Air Changes per Hour (ACH) of the ventilation system in the following way:

$$ACH = \frac{\dot{Q}}{V_{room}} = \frac{2808}{0.1125} = 6.1\frac{1}{h} \tag{4.5}$$

This level of ventilation is sufficient for normal occupancy in hospitality or recreational venues. However, it also sets a specific standard of performance for the air purification technologies being considered. Adding any air cleaning devices can't lower this ventilation rate, because less ventilation would mean worse air quality and thermal comfort.

By establishing these parameters duct geometry, hydraulic diameter, airflow rate, air velocity, available static pressure, and room volume, it is possible to model the performance of the HEPA and UVGI systems under conditions that are typical of actual HVAC installations. These reference conditions will be employed for both theoretical cases, facilitating the comparison of outcomes and enabling an equitable evaluation of the performance, spatial requirements, and operational feasibility of each system.

4.2 Case A: HEPA Filtration System

4.2.1 System Configuration

The HEPA filter studied in this theoretical analysis is designated as H14 and is characterized by a certified minimum efficiency of 99.995% at the most penetrating particle size (MPPS), typically ranging from 0.1 to 0.3 µm. This very high level of filtration efficiency makes sure that almost all particles in the air are removed, even small aerosols and biological contaminants. H14 filters are great for cleanrooms, labs, hospitals, and transportation because of this.

The filter's size was chosen to fit properly inside the ductwork because the reference HVAC system has a rectangular duct with a cross section of 450 × 250 mm. A tollerance of 2 mm on each side was considered to allow for insertion and installation, considering a nominal width, height and dept of 610 x 448 x 248 mm, ensuring sufficient sealing capacity to prevent air bypass at the edges of the filter-duct interface. Having these dimensions, we can estimate the unit volume of the filter as follows:

$$W \cdot D \cdot H = 0.610 \cdot 0.448 \cdot 0.248 = 0.068m^3 \tag{4.6}$$

Considering the internal media surface area, while the external dimensions are relatively compact, it is considerably larger because of the pleated shape of the filtration medium. From standard industrial values for HEPA filters of similar depth and weight, based on the density and number of pleats, the estimated effective media surface area will be 40 m^2. This large surface area is needed to keep the pressure drop across the filter at a reasonable level while still providing the high efficiency and dust holding capacity that is needed. The total weight of the filter is about 16.5 kg, which includes the weight of the pleated media, frame, and built-in gaskets or sealing elements. In the next sections, we will discuss the calculations and the designed parameters needed to estimate the HEPA H14 filter performance to prevent the spread of pathogens in the air.

4.2.2 Clean Air Delivey Rate (CADR)

To quantitatively estimate the improvement in indoor air quality resulting from the integration of an HEPA H14 filter, it is necessary to adopt a performance metric that not only considers the nominal airflow but also the actual amount of clean air being supplied to the space. Thus, the Clen Air Delivery Rate (CADR), which is a measure of the volume of clean air an air filtration system can deliver per unit of time, is introduced as a comprehensive metric that accounts for both the system's filtration efficiency and the actual operational conditions, including possible air leakage or imperfect installation. The CADR is calculated with the following equation:

$$CADR = \varepsilon \cdot \eta \cdot \dot{Q} \tag{4.7}$$

Where ε is the Effective Air Cleaning Ratio, η is the efficiency of the filter and $\dot{Q}$ is the volumetric airflow in m^3/h. The Effective Air Cleaning Ratio (EACR) is a non dimensional correction factor that takes account of the difference between the theoretical and actual performance of an air filtration system. The EACR's value ranges between 0 and 1, and it shows how much of the air is actually cleaned, taking into account things like air bypass, imperfect sealing, uneven airflow distribution, and mixing problems in the space that is being treated. In this study, a value of 0.765 was used because it is a common value found in the literature, which usually ranges from 0.70 to 0.83. The filter's efficiency is directly related to the filter penetration rate, which is the percentage of particles that get through the filter media. The efficiency of the filter is correlated to the filter penetration rate through the following expression:

$$\eta = 100 - P_f \tag{4.8}$$

Being P_f the penetration efficiency rate and $\eta = 99.995\%$. Lastly, we consider the volumetric airflow $\dot{Q} = 2808\ m^3/h$, as stated in the theoretical operational

data. We can now calculate the Clean Air Delivery Rate substituting the terms in the *Equation 4.8*:

$$CADR = 0.765 \cdot 0.99995 \cdot 2808 = 2148.01 m^3/h \tag{4.9}$$

After having estimated a CADR value, we can notice that the amount of the nominal airflow is higher than the CADR value, maening that only approximately 76% of the air processed by the system is effectively purified according to HEPA standards. Moreover, based on the calculated CADR, the effective Air Changes per Hour (ACH) can now be determined as follows:

$$ACH_{eff} = \frac{CADR}{V_{room}} = \frac{2148.01}{460} = 4.67 \frac{1}{h} \tag{4.10}$$

Being V_{room} the volume of the reference room considered for the air purification analysis.

4.2.3 Pressure Drop

The integration of an HEPA filter within an HVAC system introduces an inevitable pressure loss, which is caused by the resistance to airflow of the highly pleated filtering media. The pressure drop caused by the filter determines the additional mechanical energy that the ventilation system has to provide in order to maintain the required flow through the filter and in the treated space. In the present situation, the determination of the pressure drop is based on an empirical formula separating the contributions of the resistance of the filter media, the friction losses in the airflow conduits, and the localized resistances due to geometric transitions in the inlet and outlet regions.

According to the study conducted by Zhonglin Xu [1](2014), the total pressure drop ΔP can be calculated as:

$$\Delta P = \Delta P_1 + \Delta P_{2(1)} + \Delta P_{2(2)} + C \tag{4.11}$$

with

$$C = \Delta P_3 + \Delta P_4 \tag{4.12}$$

Where

[1]Zhonglin Xu (2014). Fundamentals of Air Cleaning Technology and its Application in Cleanrooms.

- ΔP_1 is the pressure drop of filter media;
- $\Delta P_{2(1)}$ is the frictional resistance of inlet passage;
- $\Delta P_{2(2)}$ is the frictional resistance of outlet passage;
- C is the local resistance of both inlet and outlet passage;
- ΔP_3 is the local resistance of inlet passage;
- ΔP_4 is the local resistance of the outlet passage.

The general expression of the pressure drop across a filtration system, as given by Xu (2014), provides a systematic decomposition of the principal contributing elements, such as the intrinsic resistance of the filter media, frictional losses in inlet and outlet flow passages, and local resistances due to sudden geometrical changes. To transform this conceptual model into an effective engineering tool for design and performance analysis, however, Xu (2014) further expands each term into an analytical expression through the inclusion of empirical coefficients, fluid properties, and geometrical parameters of the filter assembly. The resulting expression accounts for both viscous and inertial effects and allows for a more accurate calculation of the overall pressure drop as a function of airflow rate and pleat geometry. The semi empirical model thus established forms the foundation of the pressure drop calculation adopted in this case study. The expression of the total pressure drop becomes:

$$\Delta P = jA \cdot \frac{Q}{a'b'} \cdot \left(\frac{T+h}{L}\right) + 93i\mu \frac{Q}{a'b'} \cdot \left(\frac{T+h}{h^3}\right) L + C \tag{4.13}$$

With

$$a' = a - (h + T) \tag{4.14}$$

$$b' = b - 2\delta \tag{4.15}$$

Where

- $j = 1.087$;
- A is the structural coefficient or drag coefficient;
- Q is the volumetric flow rate through the air filter [m^3/s];
- a and b are the side lengths of the air filter, representing the net dimensions after subtracting the frame thickness;

- L is the depth of the air passage, i.e., the length of the corrugation line on the separator;
- f is the area of the filter media on each corrugation;
- T is the thickness of the filter media;
- δ is the depth of adhesive at both ends of the filter, including the height of the glue on the filter media or the head glue;
- C is the local resistance of both inlet and outlet passage;
- i is a dimensionless correction factor used to account for viscous effects in the pleat channels;
- μ is the dynamic viscosity.

In order to apply the full analytical expression for the pressure drop across the HEPA filtration system, a definite set of parameter values had to be determined. Taking into account the theoretical nature of this case study and the absence of overall internal specifications of the commercial filter used, a set of reasonable assumptions was created. These assumptions were led by data reported in literature, technical datasheets from filter manufacturers, and practical values observed in real HVAC installations using pleated H14 filters in similar operating conditions. Parameters such as the thickness of the filter media, the pleat height, the effective flow passage length, the dimensions of the adhesive layers, and the net active face area (after subtracting the frame width) were all set to values within the expected range for high-efficiency filters designed for duct-mounted applications. By substituting these pragmatically assumed values into the overall semi-empirical scheme described above, we were able to figure out how much pressure would drop over the filter module.

The result of this calculation was about **250 Pa**, which is very close to the initial pressure drops that were measured for clean HEPA H14 filters at standard airflow rates. This finding not only confirms the internal validity of the adopted model but also substantiates the plausibility of the assumed parameters. The calculated pressure drop was therefore adopted as a reference value for further fan power requirement and ventilation compensation analyses. Although the exact internal geometry of the filter might differ somewhat from the assumed reference geometry, the order of magnitude and airflow resistance behavior are still representative of practical applications and thus appropriate to the extent of this study. *Table 4.1* shows the theoretical values adopted for the pressure drop calculation:

Table 4.1: Assumed parameter values for theoretical pressure drop calculation

Parameter	Symbol	Value	Unit	Description
Drag coefficient	A	1.2	–	Empirical value from literature
Correction factor	j	1.087	–	From Xu (2014)
Flow rate	Q	0.5967	m^3/s	Corresponds to CADR = 2148 m^3/h
Net filter width	a'	0.448	m	Effective internal width
Net filter height	b'	0.610	m	Effective internal height
Filter media thickness	T	0.0005	m	Typical value for fiberglass media
Pleat height	h	0.0022	m	-
Pleat length	L	0.248	m	Equal to the filter depth
Dynamic viscosity of air	μ	1.8×10^{-5}	$Pa \cdot s$	At 20°C (dry air)
Local resistance	C	20	Pa	Assumed inlet/outlet loss

4.2.4 Decay Time of Particles

One of the most meaningful parameters in assessing the efficacy of a high efficiency air filtration system is the particle decay time, which measures how quickly the concentration of airborne particulate matter in a particular indoor setting decreases after the filtration system has been turned on. This is especially significant in enclosed environments like passenger ship cabins, where mechanical ventilation is the prevailing method of air exchange and contaminant elimination. An exponential model describes how particles lose concentration over time because of filtration and ventilation systems. This is called temporal decay. The model assumes that the air in the room is mixed evenly, which means that the concentration of particles is the same at all points in space and goes down evenly when clean air is added. The equation used to describe the decay time of particles is:

$$C(t) = C_0 \cdot e^{-ACH \cdot t} \tag{4.16}$$

Where

- C_0 is the initial particle concentration in the room;
- $C(t)$ is the concentration in the room at time t;
- t is the time in hours;
- ACH is the Air Changes per Hour;
- e is the Neperian number.

This formulation is derived from a first-order differential equation describing the rate of change of particle concentration in a closed environment under continuous removal, analogous to radioactive decay or first-order chemical reactions.

To illustrate the use of this model, let us consider an initial concentration of particles of C_0=1000 $\mu g/m^3$, which could represent, for instance, the number of particles per liter of air or a relative concentration index right after a contamination event.

Using the previously mentioned equation and computing the concentration of particles after 30 minutes, 1 hour and 1.5 hours, we can compute the following values:

For $t = 0.5h$:

$$C(0.5) = 1000 \cdot e^{-4.67 \cdot 0.5} = 96.81 \mu g/m^3 \tag{4.17}$$

For $t = 1h$:

$$C(1) = 1000 \cdot e^{-4.67 \cdot 1} = 9.37 \mu g/m^3 \tag{4.18}$$

For $t = 1.5h$:

$$C(1.5) = 1000 \cdot e^{-4.67 \cdot 1.5} = 0.91 \mu g/m^3 \tag{4.19}$$

Meaning that:

- After **30 minutes** ($t = 0.5h$) the concentration drops to 96.81 $\mu g/m^3$, which represent the 90.3% reduction.
- After **1 hour** ($t = 1h$) the concentration is reduced to around 9.37 $\mu g/m^3$, indicating a 99.1% reduction from the initial value.
- After **1 hour and 30 minutes** ($t = 1.5h$) the particle reduction reaches over 99.9%, effectively rendering the space virtually particle free. At this stage, the air in the environment can be considered highly purified, assuming ideal mixing and no additional particle sources.

  For a better understanding of the particles behavior over time, the graph below shows the particle reduction over the three different time periods estimated:

4.2.5 Maintenance Considerations

The addition of a high efficiency HEPA H14 filtration system in HVAC ductwork brings significant improvements to indoor air quality but at the same time places specific maintenance requirements that demand serious consideration at the system design stage, operational life cycles, and long term economic evaluation.

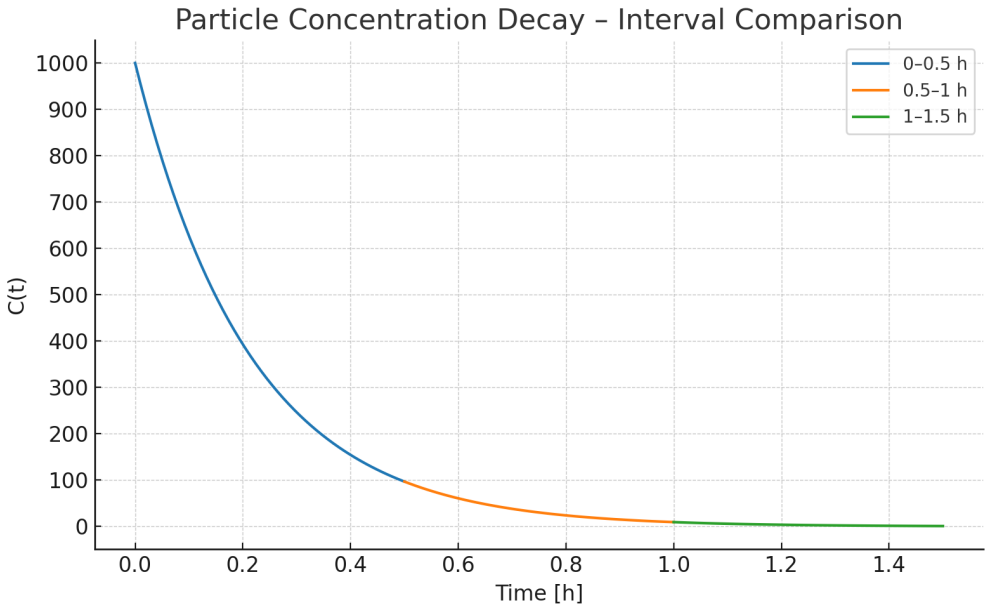

Figure 4.1: Particle concentration decay over the three time periods considered ($t = 0.5h$, $t = 1h$, $t = 1.5h$).

According to GMP (Good Manufacturing Practice) standards, there is no special maximum running time for a HEPA filter. Rather, compliance is evaluated on the basis of filter integrity, which should be leak free. Although minor repairs are permitted, they are only acceptable if the total repaired area does not exceed 0.5% of the total filter surface. While filter integrity is an important consideration, it is not the only basis to decide on replacement timing. When checking how well the filtration system is working, you should also think about the amount of particles and the drop in pressure across the filter. The ventilation system needs more energy to keep the air change rate steady as the differential pressure across the HEPA filter goes up. If the pressure drop is too high, it can go beyond what the ventilation system can handle, which can cause problems with how well it works or how efficiently it works. To fix this, pre-filters that are usually rated F7 or F9 are put in before the HEPA stage of filtering. These pre-filters are designed to catch both big and small particles, which keeps the HEPA media from getting clogged too quickly. To keep the system running well and make the HEPA filter last longer, you need to change these pre-filters every so often.

From a practical point of view, the ideal functional life of a HEPA filter is very much linked with the pressure differential. Filter replacement is required when the pressure reaches levels that either compromise the system's ability to supply the required airflow or make continued operation increasingly costly in terms of energy

consumption compared to the cost incurred in replacing the filter. For proper and regular maintenance, it is recommended to adhere to a standard checklist. Digitization of this checklist can also enhance accessibility and reliability, making it easier for maintenance crews to perform inspections and servicing activities efficiently.

According to Altomonte (january 2025), A typical HEPA filter maintenance checklist should include the following:

- Check for visible dirt accumulation, clogging, or physical damage to the filter media.
- Measure airflow resistance to detect abnormal pressure drops.
- Verify the condition of disposable pre-filters.
- Inspect the filter housing for gaps, wear, or structural damage that may lead to bypass leakage.
- Clean or assess the external surfaces for the presence of dust or contaminants that may affect system hygiene.

Besides the cost of replacing the filter directly, a big long term cost of installing a HEPA H14 filter system is the higher energy use needed to make up for the pressure drop it causes in the ventilation system. As dust and other particles build up on the filter over time, the system has to use more energy to keep the airflow going. This is because the fan has to work harder to push the air through the filter.

The annual energy cost relating to the pressure drop can be estimated using the following general equation:

$$E_{year} = \frac{\dot{Q} \cdot \Delta P \cdot t}{\eta \cdot 1000} \tag{4.20}$$

Where:

- E_{year} is the annual energy consumption [kWh/year];
- ΔP is the pressure drop across the filter [Pa];
- $\dot{Q}$ is the airflow rate [m^3/s];
- t is the total operational time in seconds per year;
- η is the overall fan efficiency (usually 0.5–0.7);

Assuming a pressure drop of $\Delta P = 250Pa$, a volumetric flow rate of $\dot{Q} = 0.5967m^3/s$, ontinuous operation (8766 hours per year), and a fan efficiency of $\eta = 0.6$, he estimated annual energy consumption becomes:

$$E_{year} = \frac{250 \cdot 0.5967 \cdot 8766}{0.6 \cdot 1000} = 2179.45kWh/year \tag{4.21}$$

If we consider an average electricity cost of €0.20 per kWh, the annual energy cost per filter installation would be approximately:

$$C_{Energy} = 2179.45 \cdot 0.20 = 435.89Eur \tag{4.22}$$

This energy expenditure repeats annually and must therefore be factored into the economic analysis of the system, particularly in large HVAC networks with many filters. Therefore, system designers and operators must find a balance between filter selection, pressure drop optimization, and energy efficiency in order to promote long term operational sustainability. Additionally, it is recommended that pressure sensors and energy measurement be integrated into the HVAC control system to allow real time performance monitoring and to adjust maintenance schedules based on actual system behavior.

4.3 Case B: UVGI Purification System

4.3.1 System Configuration

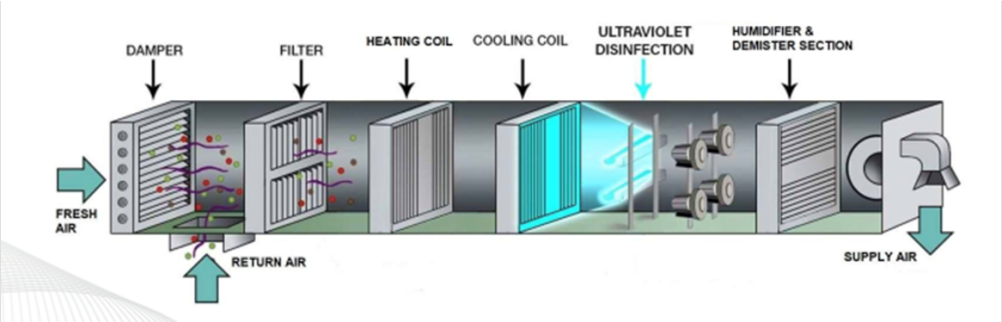

Figure 4.2: Schematic representation of a typical HVAC system with integrated UVGI disinfection unit. Source: Halton Oy study material.

The theoretical model of the UVGI (Ultraviolet Germicidal Irradiation) system considered in this case study aims to analyze both the feasibility and performance of microbial air disinfection through UV-C radiation exposure in an HVAC duct. The main goal is to model the integration of a germicidal ultraviolet system into

the air handling stream with the purpose of reducing airborne pathogen loads in a systematic and quantifiable manner. This theoretical study establishes a benchmark model to evaluate the disinfection efficacy of UVGI technology independently from other purification methods, such as mechanical filtration and chemical treatments.

The UVGI device should be placed directly in the air duct, where it will expose airborne microorganisms to short-wave ultraviolet radiation (UV-C at 254 nm), which is known to damage the DNA and RNA of bacteria, viruses, and fungi. This stops them from replicating and makes them inactive. The simulation is directed at calculating the dose delivered to the airborne pollutants in terms of irradiance and exposure time, and comparing the resulting microbial inactivation rate with standard disinfection levels, e.g., the Log3 (99.9%) reduction.

The system is designed to work under the identical airflow, duct geometry, and environmental conditions as employed in the HEPA filter example (Case A). This consistent design makes it easy to compare the two technologies directly and fairly, and it shows the pros and cons of UVGI-based purification under the same ventilation conditions. The system setup, airflow patterns, and physical assumptions are the same as they were in the last case. This lets you objectively judge how well the system works, how much space it needs, and what it means for operations. This UVGI setup doesn't have any extra filters, so it can only measure how well ultraviolet light can disinfect. This theoretical framework facilitates a comprehensive analysis of the impact of design parameters, including lamp power, irradiated length, air velocity, and duct reflectivity, on the overall efficacy of the UVGI process.

4.3.2 System settings

The UV-C lamp technology and the way the UVGI system fits into the ventilation ducting are both very important for making sure that both disinfection works and that the system works with the ventilation ducting. In the setup evaluated in this case study, the UVGI unit is designed to operate along a 2 meter long irradiated section of the HVAC duct, having a rectangular cross section of 450 mm $\times$ 250 mm. The system needs to be able to provide enough irradiance so that airborne pathogens get the right amount of UV light in the short amount of time that the airflow speed allows.

Within the given constraints, two main ultraviolet-C (UV-C) technologies are commonly considered: low pressure mercury lamps (at 254 nm) and UV-C LEDs (265–280 nm). Low-pressure mercury lamps are commonly used in industrial duct systems because they produce more germicidal power per lamp, usually between 20 and 40 watts. However, they have bulkiness, contain mercury, and require a warm up period. UV-C LEDs have several advantages in terms of their compactness,

instant turn on, and environmental friendliness. However, their individual irradiance is usually lower, so you might need more units to get the same performance.

Assuming the use of UV-C LEDs with 3 W per unit output, configured in linear arrays crosswise to the airflow, the system would need 4 to 6 LED modules for each row, spread across multiple rows along the 2 meter expanse. Module spacing and alignment need to provide even irradiance over the duct cross section area with minimal shadow areas and complete exposure of the airstream passing through.

The whole UVGI module, including the mounting frame, lamp holders, reflectors, and drivers, should have a volume that is about the same as the duct cross section (250 × 450 mm) over the full 2 m irradiated length. The total envelope of the system would thus be about 0.225 m^2 × 2 m = 0.45 m^3, not taking into account any considerations of service access or mounting clearances. The overall weight of such a system generally ranges from 8 to 14 kg and is determined by variables such as the lamp type, heat dissipation structure, and integration with the duct walls.

These factors make sure that the system can be used in ventilation ducts with the best flow performance, the least amount of pressure loss, and easy access for maintenance. Furthermore, the modular nature of LED systems allows for easy future upgrading or substitution with little requirement for large-scale changes.

4.3.3 Survival Fraction of Microbial Population Exposed to UV-C Energy

An essential step in determining the effectiveness of a UVGI (Ultraviolet Germicidal Irradiation) system is to quantify the extent to which exposure to UV-C radiation decreases the density of viable airborne microorganisms. For this purpose, a widely used model is utilized to characterize the survival fraction of a microbial population in terms of the UV dose that it receives. This relationship, widely adopted in both scientific literature and HVAC design standards, is formally presented in the ASHRAE Handbook (2024) as follows:

$$\frac{N_t}{N_0} = \exp(-k \cdot E_{\text{eff}} \cdot \Delta t) = \exp(-k \cdot \text{Dose}) \tag{4.23}$$

Where:

- N_0 is the initial number of live microorganisms;
- N_t is the number of live microorganisms remaining after exposure;
- $\frac{N_t}{N_0}$ is the fraction of surviving microorganisms (also called the survival fraction);
- k is the microorganism dependent rate constant [$\text{cm}^2/(\mu\text{W}\cdot\text{s})$];

- E_{eff} is the effective germicidal irradiance received by the microorganism [μW/cm^2];
- Δt is the exposure time to the radiation field [s];
- Dose is the product of irradiance and exposure time [μW·s/cm^2].

Having established the theoretical framework for UV-C microbial inactivation, it is essential now to evaluate all the different terms of the equation. We can now figure out how long microorganisms stay in the irradiated zone of the HVAC duct, which is called the exposure time. This parameter is directly related to the length of the irradiated zone and the speed of the airflow, assuming that the velocity profile is the same and the flow is steady.

In the configuration considered for this theoretical case, the UVGI system is installed over a duct segment with an irradiated length of:

$$L_{UV} = 2m \tag{4.24}$$

The airflow within the duct has been previously mentioned, with an air velocity of:

$$v_{air} = 9.63m/s \tag{4.25}$$

Assuming that the microorganisms are transported at the same velocity as the air and the irradiance is uniformly spread over the whole length L, the exposure time t which any airborne microbe experiences during passage through the irradiated area can be computed using the following equation:

$$t = \frac{L_{UV}}{v_{air}} = \frac{2}{9.63} = 0.208s \tag{4.26}$$

This result implies that, in the present setup, any microorganism in the air is exposed to UV-C radiation for about 0.208 seconds while passing through the system. This value will be used as a foundation for calculating the UV dose and, by extension, for approximating the disinfection effectiveness of the system.

After the exposure time is established, the second basic step is to determine the UV dose that airborne microorganisms receive while passing through the irradiated zone of the duct. The dose quantifies the total energy delivered per unit area over the exposure period and represents the most important parameter controlling the inactivation capability of the UVGI system.

The UV Dose is defined as the product of the effective germicidal irradiance and the exposure time Δt:

$$Dose = E_{eff} \cdot \Delta t \tag{4.27}$$

If I consider a theoretical effective germicidal irradiance of 54380 μW/cm^2, I can calculate the Dose as follows:

$$Dose = 54380 \cdot 0.208 = 11311.04(\mu W \cdot s)/cm^2 = 113.1 J/m^2 \tag{4.28}$$

Once the UV dose received by the air stream has been determined, the second task in determining the UVGI system's disinfection performance involves the selection of an appropriate inactivation rate constant k. This is a microorganism specific coefficient that measures the sensitivity of a specific pathogen to UV-C light. The value of k is found experimentally and is normally either measured in $[cm^2/\mu W \cdot s]$ or, in SI units as $[m^2/J]$. The larger the values of k, the more sensitive to UV the organism is, requiring a smaller dose to be inactivated. Low values of k refer to resistant organisms, e.g., spores or some bacteria.

For the purpose of this theoretical study, the following k value has been considered:

$$k = 0.0611 m^2/J \tag{4.29}$$

The chosen value here is consistent with the inactivation rate constant that was experimentally determined for SARS-CoV-2 upon exposure to UV-C light, as presented by Luo et al. (2021) in a comprehensive review of ultraviolet germicidal irradiation (UVGI) disinfection techniques. The chosen value of $k = 0.0611\ m^2/J$ represents the susceptibility of aerosolized SARS-CoV-2 in clean air settings. This selection is underpinned by the particular relevance of SARS-CoV-2 as a prominent airborne virus in enclosed environments, for example, cruise ships, where minimizing transmission via HVAC systems became an international priority during and after the COVID-19 pandemic. In addition, this virus provides a biologically relevant reference for UVGI system germicidal performance under practical operating conditions. Table 4.2 below provides a summary of the inactivation rate constants (k) for a range of airborne viruses, including coronaviruses:

We can now calculate the Survival fraction of microbial population exposed to UV-C energy substituting the know terms in *Equation 4.23*:

$$\frac{N_t}{N_0} = e^{-0.0611 \cdot 113.1} = 9.97 \cdot 10^{-4} \tag{4.30}$$

And calculating the logarithmic reduction we can obtain:

$$log_{10}(\frac{N_t}{N_0}) = -log_{10}(9.97 \cdot 10^{-4}) = 3 \tag{4.31}$$

This finding verifies that a UV dose of 113.1 J/m^2, along with an inactivation rate constant of k=0.0611 m/J for Sars-Cov-2, yields a log 3 reduction. This is

UV rate constants for coronavirus.

Phase	Coronavirus type	Paper	k (m2/J)	D_{90} (J/m2)
Liquid well plate	SARS-CoV-2	[43]	0.0611	37.7
		[44]	0.0025	921.1
		[45]	0.0188	122.5
		[46]	0.0370	62.2
	SARS-CoV	[47]	0.0181	127.3
		[48]	0.0575	40.1
		[49]	0.0008	2878.3
		[50]	0.0002	11599.9
		[51]	0.0111 (no soiling agent) 0.0091 (Mucin) 0.0099 (Sebum)	207.5 (no soiling agent) 253.1 (Mucin) 232.6 (Sebum)
		[52]	0.0093	247.6
	MERS-CoV	[53]	0.0094	244.9
		[51]	0.0104 (no soiling agent) 0.0089 (Mucin) 0.0093 (Sebum)	221.4 (no soiling agent) 258.8 (Mucin) 247.6 (Sebum)
	MHV coronavirus	[54]	0.0266 (MHV 2) 0.0190 (MHV N)	86.7 121.0
		[55]	0.0224	102.8
Aerosol	Human Coronavirus	[56]	0.41 (HCoV-229E) 0.59 (HCoV-OC43)	5.6 (HCoV-229E) 3.9 (HCoV-OC43)
	MHV coronavirus	[57]	0.377	6.1

Figure 4.3: UV rate constants for coronavirus (adapted from Luo et al., 2021)

equivalent to a 99.9% reduction of viable microorganisms, so that 0.1% of the original microbial population will remain after UV-C exposure.

The level of disinfection attained is within the commonly accepted standard for high level air sanitation in ventilation systems, especially in recirculation under confined environments such as passenger ships. The examination shows that, based on the suggested operating parameters, the UVGI system can theoretically reach high microbial inactivation using practical irradiance and exposure times, thus supporting its feasibility in HVAC applications.

4.4 Decay Time of Particles

After evaluating the disinfection efficiency of the UVGI system along the irradiated duct segment, it is possible to estimate the time to reach a log3 (99.9%) reduction in microbial concentration within the entire room environment. These calculations take into account the combined effect of both air ventilation (expressed as air changes per hour, ACH) and in-duct UVGI disinfection. The reduction of airborne microbes over time follows an exponential decay model, where the concentration at a certain time t, denoted as C(t), is expressed using the following equation:

$$C(t) = C_0 \cdot e^{-ACHtot \cdot t} \tag{4.32}$$

Where:

- $C(t)$ is the microbial concentration at time;
- C_0 is the initial microbial concentration;
- ACH_{tot} is the total Air Changes per Hour value [1/h].

This parameter includes the contribution from ventilation and the equivalent removal rate produced by UVGI, formulated as:

$$ACH_{tot} = ACH + \eta \cdot ACH \tag{4.33}$$

Where η represents the single-pass disinfection efficiency of the UVGI system, defined as:

$$\eta = 1 - e^{(-k \cdot Dose)} \tag{4.34}$$

Having the microorganism dependent rate constant $k = 0.0611\ m^2/J$, and the $Dose = 113.1\ J/m^2$, we can substitute the previously mentioned values to the equation:

$$\eta = 1 - e^{-0.0611 \cdot 113.1} = 0.999 \tag{4.35}$$

Consequently, the equivalent UVGI contribution to the total air change rate becomes:

$$ACH_{\text{UVGI}} = \eta \cdot ACH = 0.999 \cdot 6.1 = 6.09 \frac{1}{h} \tag{4.36}$$

And the ACH_{tot} can be calculated as:

$$ACH_{tot} = 6.1 + 6.09 = 12.19 \frac{1}{h} \tag{4.37}$$

Finally, the time required to achieve a Log3 reduction is calculated as:

$$\frac{C(t)}{C_0} = 0.001 \tag{4.38}$$

$$t = \frac{ln(1/0.001)}{12.19} = 0.57h \tag{4.39}$$

This result confirms that, in the chosen configuration, the UVGI system combined with ventilation, can theoretically reach the 99.9% microbial inactivation in around 34 minutes.

4.5 Eneergy Analysis

To supplement the performance evaluation of the UVGI system, an estimate of its yearly energy consumption and corresponding operating expense was conducted. The calculation is predicated on the effective irradiance needed to produce a log 3 (99.9%) inactivation of SARS-CoV-2 in the 2-meter irradiated duct segment. As calculated in earlier sections, the necessary irradiance is $E_{eff} = 543.8W/m^2$. Considering a constant irradiance over the duct cross sectional area of 0.1125 m^2(450 mm $\times$ 250 mm), the total power demand of the system is:

$$P = E_{eff} \cdot A = 543.8 \cdot 0.1125 = 61.18W \tag{4.40}$$

Considering continuous year round operation (8760 hours per year), the total annual energy consumption is:

$$E_{year} = P \cdot t = 61.18 \cdot 8760 = 535.9kWh/year. \tag{4.41}$$

By applying an average energy price of 0.20 Eur/kWh, the corresponding annual operating cost amounts to:

$$C_{Energy} = 535.9 \cdot 0.20 = 107.18Eur. \tag{4.42}$$

These findings illustrate that the energy requirement of the UVGI system is reasonably modest even with conservative continuous operation assumptions. This provides evidence for the viability of installing such systems onboard passenger ships without leading to prohibitive operating expenses, particularly when balanced against the considerable indoor air quality benefits and infection risk reduction.

4.5.1 Maintenance Considerations

The maintenance needs of UVGI (Ultraviolet Germicidal Irradiation) systems are relatively low in comparison to conventional filtration based solutions, particularly for in duct configurations. Unlike HEPA filters, UVGI systems do not capture particulate matter and thus do not undergo progressive clogging that increases pressure drop. Moreover, since the UV lamps are physically integrated within the duct, they partially block the cross sectional area of the airflow, resulting in a localized rise in air velocity and hence a small but quantifiable pressure drop. Literature estimates this extra pressure loss to be ranging between 5 and 20 Pa, depending on the quantity and geometry of lamps and supports. When UV lamps are on, they also give off heat, which adds to the heat load in the duct. Even though UVGI systems don't need to have their filters changed on a regular basis, they still need to be maintained on a regular basis to keep working as germicides. The main maintenance tasks are checking how well the lamps work, cleaning the optical surfaces to get rid of dust or moisture that could lower irradiance, and changing the UV-C lamps when they stop working. For low-pressure mercury lamps, the life of the lamp is usually between 8,000 and 12,000 hours. For UV-C LED modules, the life of the lamp can be as long as 25,000 to 30,000 hours. Cleaning is a simple process often involving wiping of lamp surfaces with rubbing alcohol while the system is turned off. Most manufacturers recommend maintenance once a year or once every two years, which can be planned around the larger HVAC service schedules. The National Institute of Health says that installing in a standard 50 m^2 space will cost between €1300 and €1700, depending on how many lamps, control systems, and mounting structures are needed.

From an operational standpoint, UVGI systems offer several advantages:

- Lower maintenance frequency compared to mechanical filtration
- Continuous inactivation of airborne pathogens during system operation
- No handling of contaminated filters or particulate waste
- Modular design with easy integration in ductwork

Nevertheless, certain limitations should be noted. Along with the pressure drop and heat generation, certain UV lamps, particularly those with wavelengths less than 240 nm, can generate ozone (O_3). For indoor air treatment, ozone free UV-C sources are highly recommended. Also, there need to be enough safety features in place to keep maintenance workers from being directly exposed to UV-C light. This can be done with interlocks, light traps, and secure housings. In conclusion, UVGI systems represent a low maintenance and technically viable solution for continuous air disinfection in HVAC ducts, as long as pressure losses, thermal

effects, lamp aging, and safety protocols are appropriately addressed during design and operation.

Chapter 5

Aero Quattro AirForte Technology

5.1 System's Description

The Aero Quattro system, developed by AirForte, is an advanced four-stage air purification technology, tailored to be integrated into HVAC systems on passenger ships. Unlike traditional solutions based solely on mechanical filtration or ultraviolet disinfection, which are respectively characterized by high pressure losses and the necessity of multiple recirculation cycles in order to obtain appreciable effects, the Aero Quattro is designed as a multi barrier device able to obtain effective purification in a single pass. Its uniqueness consists in the possibility to inactivate airborne contaminants with a Log3 reduction (i.e., 99.9% inactivation) in a single passage through the device, without requiring multiple circulation and without introducing any significant aerodynamic resistance or toxic byproducts into the ventilation system. Structurally, the Aero Quattro unit is compact and modular, ensuring adaptability to existing ductwork. The standard measurements for a single module are 460 mm in width, 480 mm in height, and 710 mm in length, excluding the mounting flanges, while its weight is around 40 Kg. In spite of this relatively small size, one unit can treat an airflow of around 400 m^3/h, with a 99.9% microbial inactivation rate per pass. Where larger volumes of air need to be treated, several Aero Quattro devices may be mounted either in parallel, to augment the treated flow capacity, or in series, if duct geometry does not allow the parallel configuration. For instance, in a ventilation duct with a cross-sectional area of 1 m^2 and an air flow of 4000 m^3/h, it is possible to place five Aero Quattro modules near the air handling unit to treat 2000 m^3/h of recirculated air. This is a typical practice on board passenger ships, where no more than 50% of the extracted air is usually reintroduced as recirculation. In *Figure 5.1* below, it is

possible to see the structure of the Aero Quattro technology deivce:

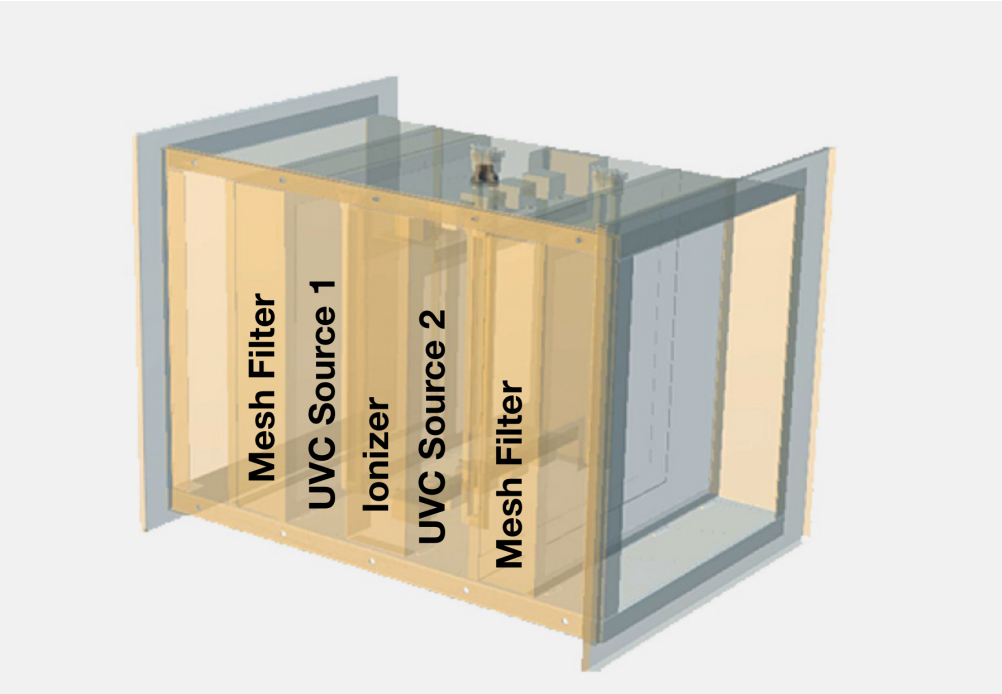

Figure 5.1: Internal configuration of the Aero Quattro air purification unit. Adopted from Duplissy (2022).

The inner setup of the Aero Quattro is extremely versatile and can be modified according to the environmental needs. The reaction chamber has two filter positions that can be fitted with various media, such as photocatalytic meshes, mechanical filters (G4, F7, HEPA), activated carbon filters, or chemical filters for specific gases like formaldehyde or volatile organic compounds.

The process of purification includes a number of steps that happen one after the other. The first step is bipolar ionization, which sends a lot of positive and negative ions into the air stream. The ions come into contact with suspended particles and microorganisms and disrupt their membranes, induce agglomeration, and decrease their viability. The airflow is then exposed to UV-C irradiation, which is a direct germicidal agent by disrupting the nucleic acids of microorganisms and, at the same time, acts as a catalyst for the next photocatalytic oxidation step. In this phase, the UV-C activation of the photocatalytic meshes produces highly reactive oxygen species, the most significant of which are hydroxyl radicals, capable of oxidising volatile organic compounds and breaking down organic pollutants into harmless by-products like carbon dioxide and water. When required, the Aero Quattro may also be equipped with mechanical filters, allowing the physical capture

of particulate matter down to submicron sizes.

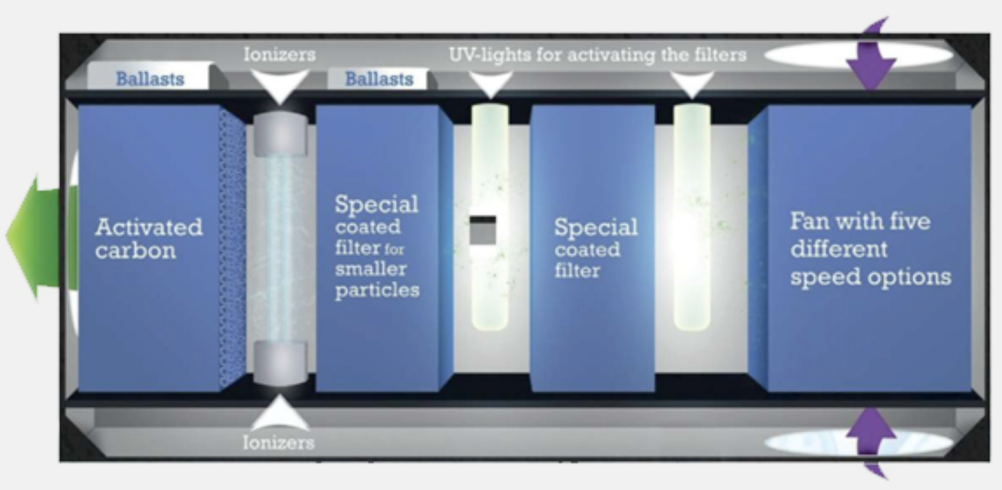

Figure 5.2: Aero Quattro internal setup. Adopted from Halton Oy official website. Avaiable at: https://www.halton.com/ (accessed 2 May 2025)

Although the Aero Quattro unit has two filter positions that can be fitted with various media, such as photocatalytic, mechanical (G4, F7, HEPA), activated carbon, or chemical filters for special gases like formaldehyde and VOCs, for the purpose of this study, both positions are considered with photocatalytic filters only, since these introduce a negligible pressure loss. As a result, no additional pressure drop has been included in the system analysis. In *Figure 5.3* below it is possible to see the technical dimensions of the Aero Quattro device unit:

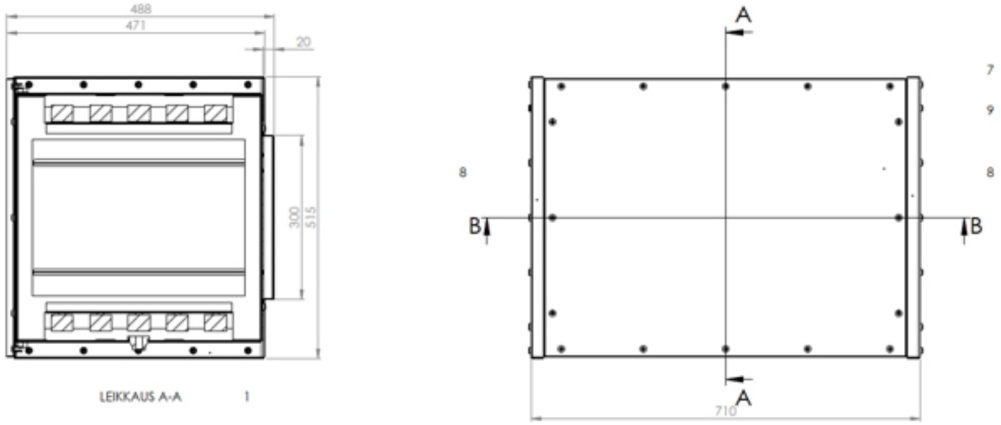

Figure 5.3: Dimensions of the Aero Quattro device unit. Adopted from Halton technical data sheet.

5.2 Experimental Performance of the Aero Quattro Technology

To evaluate the effectiveness of the Aero Quattro technology under real operating conditions on board a passenger ship, an experimental study was carried out in 2022 on board a cruise ferry sailing between between Turku in Finland and Stockholm in Sweden. This study was performed by Duplissy et al. from the University of Helsinki in collaboration with AirForte, with the objective of quantifying the effectiveness of the Aero Quattro system in deactivating airborne viruses while investigating the possible production of secondary pollutants, such as ultrafine particles or ozone. Although this vessel is not the subject of the present case study, the findings of this experimental validation provide essential reference data for evaluating the effectiveness of Aero Quattro when installed on the reference passenger vessel. During the experiment, standard mechanical filters, such as HEPA or F7, were purposely excluded. This setup allowed a larger amount of virus to pass through the device, thus allowing a determination of its disinfection efficiency under more demanding conditions, while also avoiding any pressure drop normally caused by mechanical filters.

The experimental setup of choice was carried out in a conference room aboard the ferry of volume:

$$V_{room} = (L \cdot W \cdot H) = 9.48 \cdot 5.23 \cdot 2.51 = 124.45 m^2 \tag{5.1}$$

Which was separated from the rest of the HVAC system to provide controlled conditions and prevent cross contamination of the virus to other parts of the ship. The Aero Quattro device was mounted directly into the supply air duct of the test room, and a controlled airflow of:

$$\dot{Q}_{air} = 0.38 m^3/s = 1368 m^3/h \tag{5.2}$$

was provided during the experiments to consider real ventilation conditions. For simulating viral contamination, the bacteriophage Phi6 was employed as a surrogate for enveloped viruses like SARS-CoV-2. Phi6 is an accepted model virus for aerosol transmission studies because of its morphological and structural similarity to coronaviruses, while being non pathogenic and safe for experimental use.

During experimental test, a nebuliser was used to introduce aerosolised Phi6 viruses in the airstream prior to the Aero Quattro device. Then, the infected airstream passed through the device and was sampled downstream using biosamplers for quantitative analysis.

5.2.1 Experimental Procedure

The experimental test was organized into a sequence of four control runs and four test runs, each of ten minutes duration, spread over two separate cruises. For the control runs, the Aero Quattro apparatus was turned off, allowing aerosolized viruses to be introduced into the ventilation system. This allowed their duration and transmission in untreated air to be measured. Each control run was followed immediately by a corresponding test run where the Aero Quattro was turned on under identical environmental conditions, allowing a direct comparison of treated and untreated air. During the experiments, the background aerosol concentration inside the ventilation system remained stable at approximately 4000 particles per cm^3. When the nebuliser was turned on to supply virus containing aerosols, the concentration increased to about 30,000 particles per cm^3, thus attesting to the uniformity of viral aerosolisation for all tests. Importantly, no detectable differences were found in the downstream particle size distribution of the Aero Quattro in both ON and OFF conditions. Information from the Condensation Particle Counter (CPC) and Differential Mobility Particle Sizer (DMPS) agreed that the total particle concentration returned to its background level of about 4000 particles per cm^3 between nebulisation periods regardless of the operating state of the Aero Quattro. These findings showed that the activation of the Aero Quattro did not promote the formation of ultrafine particles. Moreover, in a separate test campaign, there was no detection of ozone generation when the Aero Quattro was operating, thus confirming the absence of harmful byproducts during purification.

In this study, two different assay techniques were used to measure viral concentration:

- **qRT-PCR**, which measured the total number of viruses that can pass (viable and inactive ones) through Aero Quattro;
- **Plaque Assays**, which measures the number of infectious viruses.

This dual approach allowed the researchers to distinguish between the simple passage of virus particles through the device and their actual infectivity after treatment.

5.2.2 Virological Results

Although qRT-PCR analyzed all samples successfully, the plaque assay yielded results for around 50% of the runs collected, with some of the control and test samples being below assay limits (control runs 2, 3, and 4 in the first cruise; control run 3 in the second cruise; and test runs 1, 2, and 4 in the first cruise, and test run 4 in the second cruise).

The viral loads as measured by qRT-PCR in both control and test samples were invariably higher than those obtained using plaque assays. In the control samples, the discrepancy between the two assays was usually 2.0–2.5 orders of magnitude, due to the fact that qRT-PCR detected both viable and inactivated viruses. In the test runs, this gap increased to 3–4 orders of magnitude, showing that while viral genomes were still detectable downstream of the Aero Quattro, most of them were non infectious. Quantitatively, the Aero Quattro under ON conditions decreased the density of total viral particles by roughly one order of magnitude, as reflected in qRT-PCR calculations. However, if only infectious viruses as determined by plaque assay are considered, the decrease amounted to nearly three orders of magnitude, representing a 99.9% inactivation efficiency. Moreover, in a single test sample, the concentration of infectious viruses downstream of the Aero Quattro was lowered to zero, below the assay's detection limit, thus directly demonstrating complete viral neutralisation under these conditions.

Together, these results show that the Aero Quattro system inactivates infectious airborne viruses in a single pass with an average Log3 reduction while also avoiding the generation of unwanted secondary aerosols or ozone. From an engineering perspective, this confirms the suitability of the device for shipboard HVAC systems, where maintaining the quality of safe air is critical, but where constraints on available space, power consumption, and pressure budgets present stringent limitations. More generally in terms of health and safety, the incorporation of sophisticated air purification systems like Aero Quattro into cruise ship ventilation systems can significantly minimize risks of airborne viral transmission and thereby increase passenger safety and resilience to future outbreaks.

5.3 Aero Quattro Technology and Theoretical Case Comparison

The results from the theoretical analysis of Case A (HEPA filtration) and Case B (UVGI irradiation) provide a significant benchmark for critically evaluating the performance of Aero Quattro technology. Both HEPA filters and UVGI systems are well known ways to clean the air, but using them in cruise ship ventilation systems has big issues with pressure drop, energy use, and the range of pollutants they can remove. The Aero Quattro system, on the other hand, combines the best parts of both methods while eliminating their critical drawbacks.

Compared to the theoretical Case A, which considered the exclusive use of a HEPA H14 filter, the Aero Quattro system has clear advantages from both an operational and aerodynamic point of view. In the HEPA configuration, the filter pressure drop was estimated to be in the range of 200–250 Pa. This resistance level necessarily increases the load on the fans, either reducing the effective airflow rate

or requiring a more powerful ventilation unit, which in turn results in higher capital and operating costs. On the other hand, the Aero Quattro was tested in this study with the use of photocatalytic meshes only, with no measurable additional pressure loss. This implies that the device integration does not interfere with the airflow balance of the HVAC system and does not require any recalibration or resizing of fan capacity. The lack of measurable pressure drops leads directly to lower energy use, lower operating costs, and easier system integration.

From a maintenance point of view, HEPA filters need to be changed regularly every 6 to 12 months under typical conditions, and their disposal needs to be carefully handled since loaded filters can retain biological contaminants. This not only represents ongoing operational costs but also safety issues with respect to waste handling. The Aero Quattro, in contrast, has just annual maintenance, with replacement of UV-C sources and ionisation modules, both of which are designed for long life. No hazardous waste is produced, and no consumables comparable to large filter elements are required. It results in significantly lower maintenance costs and downtime over the operating life of the vessel.

The comparison with Case B, based on a UVGI only system, highlights further strengths of Aero Quattro. Although UVGI irradiation is effective at microbial load reduction, its effectiveness is heavily dependent on exposure time and irradiance. In the theoretical study, a Log3 reduction was attained after about 34 minutes of operation, relying on adequate residence time in a two meter irradiated duct section. Such a solution, however, demands substantial space, high lamp density, and high electrical consumption, which cumulatively enhance installation complexity as well as long-term expense. Moreover, traditional UVGI systems predicated on mercury lamps carry the potential for ozone generation, which is unacceptable in occupied spaces. Aero Quattro, in contrast, was able to achieve a Log3 inactivation in a single pass, lowering the concentration of infectious viruses by 99.9% without necessitating multiple cycles of circulation through the unit. Laboratory tests also revealed that the device generates zero ozone or ultrafine particles when in operation, guaranteeing absolute safety for continuous operation on board.

Finally, the Aero Quattro combines the best features of both theoretical cases into one device, making it the best choice offered by both theoretical cases. Like the HEPA filter, it allows for the removal of particulate matter without suffering from considerable aerodynamic penalties. At the same time, like the UVGI system, it efficiently inactivates microorganisms, doing so with even better efficiency through single pass treatment and without generating harmful byproducts. In addition, using photocatalytic oxidation, it reduces volatile organic compounds and odours, thereby extending its purification range beyond that of Case A and Case B. Taken together, these advantages translate to improved efficiency, lower operating costs, and simplified maintenance, making the Aero Quattro a more effective and sustainable solution for ventilation systems on passenger ships.

5.4 Integration of Aero Quattro Units: Space Analysis and Configuration of AC room 25

The installation of the Aero Quattro technology on board the reference passenger vessel requires a careful evaluation of the available space in the ship's HVAC system. The selected location for the installation of the Aero Quattro devices is the AC Room 25, located on Deck 12, which houses a portion of the ship's ventilation ductwork and allows access for system modification and maintenance. As part of the project, a representative technical room was taken into account, which represents the spatial proportions and characteristics of a ventilation duct appropriate for this investigation. This environment served as the basis for assessing the potential for implementing the Aero Quattro system.

Figure 5.4: Frontal view of the ventilation duct in AC Room 25 (Deck 12, reference passenger vessel)

The measured duct dimensions in AC room 25 are: 50 cm in width and 100 cm in length, with a vertical clearance of 70 cm from the base of the duct to the ceiling connection. Furthermore, the surrounding clearances were also recorded: laterally, the duct edge is located at a distance of approximately 30 cm from the adjacent wall, while in the longitudinal direction, a free space of 2 metres extends from the end of the duct section to the room's rear wall. This configuration ensures sufficient accessibility for the installation of auxiliary devices, as well as for subsequent maintenance interventions. The figures below show the measurements taken during the site inspection of the reference passenger vessel:

A comparison of the two sets of dimensions indicates that the Aero Quattro unit is slightly smaller than the cross section of the duct (duct: 50 × 70 cm vs. unit: 46 × 48 cm). This means the device can fit comfortably inside the duct without major modifications. If necessary, small mounting frames or adapters could be used to secure the unit and ensure airtight sealing.

The Aero Quattro is 71 cm long, and the duct is 100 cm long, with a 29 cm margin. This margin, along with the 2 m free clearance downstream, shows that there is enough room for installation and for maintenance access later on. This spatial assessment confirms that the unit can be added to the current duct system without making major changes to the structure. The best way to set up the system is in parallel, taking into account the size of the space and the need to maximize airflow while minimizing overall pressure losses. This setup makes sure that the device works well in the small space of AC Room 25, is easy to get to for maintenance, and meets ventilation performance standards.

Chapter 6

Conclusions and Perspectives

This study investigated the challenge of maintaining high levels of indoor air quality (IAQ) on passenger vessels, analyzing the incorporation of different purification technologies into shipboard HVAC systems. Based on a comprehensive literature review and technical analysis, traditional filtration and disinfection methods, such as HEPA filters and ultraviolet germicidal irradiation (UVGI) systems, were compared to a new air purification system: the Aero Quattro module developed by AirForte Oy. Theoretical performance tests of both UVGI and HEPA systems were conducted with theoretical duct data and simulation assumptions. These theoretical scenarios emphasized the characteristic advantages and disadvantages of each system. Through a detailed state of the art review and technical analysis, the implementation of an Hepa H14 class filter into the maritime HVAC systems is constrained by high pressure drops, compromising energy efficiency, and high maintenance requirements for filter replacement and airflow monitoring. UVGI systems, although effective at microbial inactivation, necessitate large volumes of installation space, high power consumption, and tight densities of UV lamps to be efficient in a single pass scenario. These limitations make UVGI systems less practical for retrofitting ships, especially when we consider the thermal load, limited space, and risk of ozone generation that comes with using a good amount of UV. The Aero Quattro module, however, stood out as the most promising alternative among the technologies reviewed. Performance measurements from installations on Viking Line ships show that the system operates in a single pass mode, meaning that the air purification is effected by a single pass through the unit unlike traditional systems which require multiple circulations to reach similar efficacy. This aspect, combined with a low pressure drop of around 20 Pa, makes the system very compatible with existing ventilation systems, with no requirement

for additional fan power or system recalibration. Additionally, the Aero Quattro system is an ozone free device, unlike many ionization or low wavelength UV based systems, and it requires minimal maintenance, as it does not depend on filter media that need regular replacement. The Aero Quattro system's modular four stage design is another important benefit. This lets it be customized to meet the needs of different operational environments and indoor air quality. This kind of flexibility is especially useful in marine settings, where the number of people, the amount of humidity, and how the compartments are used can all be very different.

The Sunflower Pool Area, a high humidity wellness area on Deck 12, was chosen as the target area for the Aero Quattro unit to service the reference passenger vessel. A key component of this thesis was the space management analysis conducted in the AC Room 25, the technical room tasked with supplying air to the Sunflower Pool Area through AC232. System layout measurements and evaluations resulted in the choice of a parallel configuration for the installation of the Aero Quattro, which was found to be the most effective and least obtrusive arrangement, providing ample clearance for maintenance and working safety. Although the Aero Quattro system is not yet physically installed on the reference passenger vessel, this thesis relies on installation data from an external experimental study conducted on a cruise ferry operating the Turku–Stockholm route, which is used as a performance benchmark to estimate its behavior in the designated onboard environment. This made it possible to conduct a realistic pre installation analysis of airflow compatibility, pressure demands, purification potential, and energy consumption efficiency.

6.1 Critical Reflection and Future Evolution of the Research

While the results obtained in this study confirm the technical feasibility and comparative advantages of the Aero Quattro system, it is essential to interpret these findings within a forward looking perspective. Rather than limiting the discussion to the specific case study analyzed, the research opens several avenues for future development that can strengthen and expand its impact.

A natural continuation of this work would involve the full scale onboard implementation of the Aero Quattro module within the selected reference vessel, followed by systematic monitoring under real operational conditions. Such an implementation would allow validation across seasonal variations, fluctuating passenger densities, and dynamic HVAC operating modes. This step would not aim to question the findings presented here, but to reinforce them through longitudinal empirical evidence, transforming pre installation projections into documented operational benchmarks. Beyond validation, the research could evolve toward integration with smart control architectures. Modern ships increasingly rely on

digital management systems capable of adjusting ventilation parameters in response to occupancy levels and environmental sensors. Incorporating the Aero Quattro technology within a feedback driven control loop could optimize purification intensity according to real time indoor air quality indicators. This would shift the paradigm from static purification to adaptive air management, enhancing both health protection and energy efficiency. Another dimension of future development concerns the broader applicability of the Aero Quattro concept beyond maritime environments. The characteristics identified in this thesis low pressure drop, single pass effectiveness, compact design, and modular scalability are highly relevant in other high density transportation sectors. Aircraft cabins, for example, operate under strict spatial and weight constraints while maintaining partial recirculation strategies. A lightweight, aerodynamically efficient purification module inspired by the Aero Quattro architecture could potentially reduce maintenance cycles and optimize airflow resistance within aircraft environmental control systems. Similarly, high speed trains, metro systems, and long distance buses represent enclosed environments where recirculation is often necessary for energy reasons. In such contexts, technologies capable of delivering effective single pass purification without imposing substantial pressure losses could enhance passenger safety without increasing operational costs. The potential applications extend even further to healthcare facilities, underground infrastructures, temporary emergency shelters, and modular accommodation units. In environments where recirculation is limited or external air intake is constrained, a compact multi stage purification unit may complement existing ventilation strategies and provide decentralized air treatment solutions. The Aero Quattro system therefore represents not only a product solution, but a design philosophy centered on balanced performance optimization. At regulatory level, the findings of this thesis may contribute to future discussions on performance based indoor air quality standards in maritime and transportation sectors. As public awareness regarding airborne transmission increases, regulatory frameworks may progressively incorporate specific microbial reduction targets or contaminant concentration thresholds. Technologies that combine high purification efficiency with minimal system impact are well positioned to support such evolution. From a sustainability perspective, the low pressure drop characteristic of the Aero Quattro unit may indirectly contribute to decarbonization strategies by reducing auxiliary energy consumption associated with ventilation systems. In large passenger vessels, even marginal reductions in fan power demand can translate into meaningful lifecycle energy savings. The alignment between health protection and energy efficiency represents a critical direction for future HVAC innovation.

6.2 Aspects Requiring Further Investigation

Although the present study provides a solid technical foundation, several aspects deserve deeper exploration in subsequent research phases. One area for further investigation concerns comprehensive multi contaminant performance assessment. While this thesis primarily focused on biological risk mitigation, future studies could integrate chemical pollutant removal efficiency, volatile organic compound reduction, and fine particulate behavior under varying humidity conditions. A holistic IAQ evaluation framework would strengthen the multidimensional performance characterization of advanced purification systems. Another promising direction involves detailed airflow distribution modeling through computational fluid dynamics simulations. Such analyses could provide high resolution insight into aerosol dispersion patterns within complex shipboard geometries, enabling optimization of diffuser placement and purification module positioning. Lifecycle sustainability assessment also represents an important extension. Evaluating manufacturing footprint, operational energy consumption, maintenance logistics, and end of life considerations would provide a comprehensive environmental profile of the technology. Finally, cross sector comparative studies could explore how the Aero Quattro architecture performs under the operational constraints of aviation, rail transport, and healthcare facilities. Such benchmarking would position the system as a reference model for next generation air purification solutions.

6.3 Concluding Perspectives

The Aero Quattro system emerges from this investigation as a technologically mature and strategically promising solution. Its modular design, low pressure drop, ozone free operation, and adaptability to diverse environmental conditions make it particularly suited for integration within complex transportation infrastructures. Looking ahead, the continuation of this research should move toward integrated, adaptive, and performance based air management systems capable of responding dynamically to changing environmental conditions. In this context, the Aero Quattro concept may serve not only as a specific technological solution for maritime HVAC systems, but as a benchmark architecture for future indoor air quality strategies across transportation and high density enclosed environments. In conclusion, the present work contributes both scientifically and practically to the advancement of air purification integration in passenger vessels. By combining rigorous comparative analysis with applied feasibility assessment, the thesis lays a strong foundation for future developments in health centered, energy efficient ventilation design.

Bibliography

[1] Olivier Schalm, Gustavo Carro, Borislav Lazarov, Werner Jacobs, and Marianne Stranger. «Reliability of Lower-Cost Sensors in the Analysis of Indoor Air Quality on Board Ships». In: *Atmosphere* 13.10 (2022), p. 1579. DOI: 10.3390/atmos13101579.

[2] Orouba Almilaji. «Air Recirculation Role in the Spread of COVID-19 Onboard the Diamond Princess Cruise Ship during a Quarantine Period». In: *Aerosol and Air Quality Research* (2021). DOI: 10.4209/aaqr.200495.

[3] *Ships and marine technology - Air-conditioning and ventilation of accommodation spaces and other enclosed compartments on board ships - Design conditions and basis of calculations*. Standard. International Organization for Standardization, Apr. 2022.

[4] Davide Truffo, Josè Miguel Peña Suarez, Juan Bandera Cantalejo, Maria Del Carmen Gonzalez Muriano, Francisco Garcias Vacas, and Francisco Fernandez Hernàndez. «Comparative study of purifications technologies and their application to HVAC systems». In: *E3S Web of Conferences*. Vol. 343. E3S Web of Conferences. 2022, p. 03005. DOI: 10.1051/e3sconf/202234303005.

[5] *Transmission of SARS-CoV-2: implications for infection prevention precautions*. World Health Organization. July 2020. URL: https://www.who.int/news-room/commentaries/detail/transmission-of-sars-cov-2-implications-for-infection-prevention-precautions (visited on 04/18/2025).

[6] *What Is a HEPA Filter & How Does It Work?* ISO-Aire. URL: https://www.iso-aire.com/blog/what-is-a-hepa-filter-and-how-does-it-work (visited on 03/12/2025).

[7] Maryam Zahaba et al. «Indoor air quality (IAQ) in a naval ship after refit program: a time variation analysis». In: *IOP Conference Series: Earth and Environmental Science*. Vol. 1013. IOP Conference Series: Earth and Environmental Science 1. 2022, p. 012004. DOI: 10.1088/1755-1315/1013/1/012004.

[8] *2024 ASHRAE Handbook: Heating, Ventilating, and Air-Conditioning Systems and Equipment*. SI Edition. Peachtree Corners, GA: ASHRAE, 2024. ISBN: 9781955516846.

[9] Evangelia Chrysikou, Eva Hernandez Garcia, and Eleftheria Savvopoulou. *International Research Project on Emergency Response to Infectious Disease Outbreak on Cruise ships*. Tech. rep. The Bartlett Real Estate Institute, University College London, 2021.

[10] Buddhi Pushpawela, Rohan Jayaratne, Aline Nguy, and Lidia Morawska. «Efficiency of ionizers in removing airborne particles in indoor environments». In: *Journal of Electrostatics* 90 (2017), pp. 79–84. DOI: 10.1016/j.elstat.2017.10.002.

[11] Federico Noris, Jeffrey A. Siegel, and Kerry A. Kinney. «Evaluation of HVAC filters as a sampling mechanism for indoor microbial communities». In: *Atmospheric Environment* 45.2 (2011), pp. 338–346. DOI: 10.1016/j.atmosenv.2010.10.021.

[12] Jing Wu, Jiawei Chen, Jason S. Olfert, and Lexuan Zhong. «Filter evaluation and selection for heating, ventilation, and air conditioning systems during and beyond the COVID-19 pandemic». In: *Indoor Air* 32.9 (2022), e13099. DOI: 10.1111/ina.13099.

[13] M. S. Waring and J. A. Siegel. «Particle loading rates for HVAC filters, heat exchangers, and ducts». In: *Indoor Air* 18.3 (2008), pp. 209–224. DOI: 10.1111/j.1600-0668.2008.00518.x.

[14] Xin Zhang, Junjie Liu, Xuan Liu, Chaojun Liu, and Qingyan Chen. «HEPA filters for airliner cabins: State of the art and future development». In: *Indoor Air* 32.10 (2022), e13103. DOI: 10.1111/ina.13103.

[15] Bingbing Shi, Lars E. Ekberg, and Sarka Langer. «Intermediate Air Filters for General Ventilation Applications: An Experimental Evaluation of Various Filtration Efficiency Expressions». In: *Aerosol Science and Technology* 47.5 (2013), pp. 488–498. DOI: 10.1080/02786826.2013.768078.

[16] *Method of Testing General Ventilation Air-Cleaning Devices for Removal Efficiency by Particle Size*. Standard. ASHRAE, 2017.

[17] Olivier Schalm, Gustavo Carro, Werner Jacobs, Borislav Lazarov, and Marianne Stranger. «The Inherent Instability of Environmental Parameters Governing Indoor Air Quality on Board Ships and the Use of Temporal Trends to Identify Pollution Sources». In: *Indoor Air* 2023 (2023), p. 7940661. DOI: 10.1155/2023/7940661.

[18] Jun Guan, Yabin Jia, Zhiyi Wei, and Xiufeng Tian. «Temporal variations of ultrafine particle concentrations in aircraft cabin: A field study». In: *Building and Environment* 153 (2019), pp. 1–10. DOI: 10.1016/j.buildenv.2019.02.025.

[19] Teresa M. Mata, António A. Martins, Cristina S. C. Calheiros, Florentina Villanueva, Nuria P. Alonso-Cuevilla, Marta Fonseca Gabriel, and Gabriela Ventura Silva. «Indoor Air Quality: A Review of Cleaning Technologies». In: *Environments* 9.9 (2022), p. 118. DOI: 10.3390/environments9090118.

[20] Manuel Armando Atancuri and Juan-Carlos Cobos-Torres. «Ionization Air Purifying Lattice Prototype». In: *Buildings* 13.3 (2023), p. 634. DOI: 10.3390/buildings13030634.

[21] Holger Claus. «Ozone Generation by Ultraviolet Lamps». In: *Photochemistry and Photobiology* 97 (2021), pp. 471–476. DOI: 10.1111/php.13391.

[22] Salvador Escobedo and Hugo de Lasa. «Photocatalysis for Air Treatment Processes: Current Technologies and Future Applications for the Removal of Organic Pollutants and Viruses». In: *Catalysts* 10.9 (2020), p. 969. DOI: 10.3390/catal10090969.

[23] Daniel Jones and Michael Ivanovich. «UV-C for HVAC Air and Surface Disinfection». In: *inmotion (pubblicato tramite ResearchGate)* (Oct. 2020).

[24] Brent Stephens, Elliott T. Gall, Mohammad Heidarinejad, and Delphine K. Farmer. «Interpreting Air Cleaner Performance Data». In: *ASHRAE Journal* (Apr. 2022), pp. 20–31.

[25] *Buildings.Examples.VAVReheat - Modelica Buildings Library*. Lawrence Berkeley National Laboratory. URL: https://simulationresearch.lbl.gov/modelica/releases/v4.0.0/help/Buildings_Examples_VAVReheat.html.

[26] Niklas Korja. «Measured and experienced indoor environmental quality on a cruise ship (Titolo tradotto dal finlandese: Mitattu ja koettu sisäympäristön laatu risteilylaivalla)». MA thesis. Aalto University, Feb. 2024.

[27] Martin Kiil, Alo Mikola, Karl-Villem Võsa, Raimo Simson, and Jarek Kurnitski. «Ventilation effectiveness and incomplete mixing in air distribution design for airborne transmission». In: *Building and Environment* 267 (2025), p. 112207. DOI: 10.1016/j.buildenv.2024.112207.

[28] DNV. *Aerosol Distribution and Transmission Supported by Ventilation Systems*. Tech. rep. DNV, Mar. 2021.

[29] *Filtration Techniques: Which filtration techniques can improve virus protection in HVAC systems?* Tech. rep. Whitepaper. 2020.

[30] *Recommendations from the Healthy Sail Panel: Advice to cruise operators to advance their public health response to COVID-19...* Tech. rep. Sept. 2020.

[31] *REHVA COVID-19 Ventilation Calculator documentation (version 2.0, August 1, 2021)*. Tech. rep. Sept. 2021.

[32] *Criteria for room air cleaners for particulate matter: Recommendation from the Nordic Ventilation Group*. Tech. rep. Data di pubblicazione non specificata.

[33] W. J. Kowalski and William P. Bahnfleth. «UVGI Design Basics for Air and Surface Disinfection». In: *HPAC Engineering* (Jan. 2000), pp. 100–110.

[34] *Advanced Oxidation Test Results 2000-2016*. Test Booklet. 2016.

[35] *AERO 1000 BM-FP*. Scheda tecnica prodotto. ITALYDRY.

[36] *Chapter 62: Ultraviolet Air and Surface Treatment*. ASHRAE, 2019.

[37] Wladyslaw Jan Kowalski. «Design and Optimization of UVGI Air Disinfection Systems». PhD thesis. The Pennsylvania State University, Aug. 2001.

[38] Jeremy B. Dreiling. «An Evaluation of Ultraviolet Germicidal Irradiation (UVGI) Technology in Health Care Facilities». MA thesis. Kansas State University, 2008.

[39] Jamie Trahan, Alessandro Graziani, D. Yogi Goswami, E. Stefanakos, Chand Jotshi, and Nitin Goel. «Evaluation of pressure drop and particle sphericity for an air-rock bed thermal energy storage system». In: *2013 ISES Solar World Congress*. Vol. 57. 2014, pp. 633–642. DOI: 10.1016/j.egypro.2014.10.219.

[40] Zhonglin Xu. *Fundamentals of Air Cleaning Technology and Its Application in Cleanrooms*. Berlin, Heidelberg: Springer, 2014. ISBN: 978-3-642-39374-7.

[41] *Product catalogue 2015*. Product Catalog. 2015.

[42] *HEPA/ULPA Filters, Class H10 to U17*. Product Data Sheet. Camfil Farr.

[43] *DHL HEPA terminal filter diffuser*. Product Data Sheet DHL/0313/EN. Halton, 2013.

[44] Kwang-Chul Noh and Se-Jin Yook. «Evaluation of clean air delivery rates and operating cost effectiveness for room air cleaner and ventilation system in a small lecture room». In: *Energy and Buildings* 119 (2016), pp. 111–118. DOI: 10.1016/j.enbuild.2016.03.030.

[45] R. L. Peck, S. A. Grinshpun, M. Yermakov, M. B. Rao, J. Kim, and T. Reponen. «Efficiency of portable HEPA air purifiers against traffic related combustion particles». In: *Building and Environment* 98 (2016), pp. 21–29. DOI: 10.1016/j.buildenv.2015.12.014.

[46] W. Bergman, M. W. First, W. L. Anderson, H. Gilbert, and J. W. Jacox. «Criteria for Calculating the Efficiency of HEPA Filters During and After Design Basis Accidents». In: *Proceedings of the 23rd DOE/NRC Nuclear Air Cleaning and Treatment Conference*. Preprint UCRL-JC-119490. July 1994.

[47] Ken A. Smigielski. «Design and Setup of a System for Testing HEPA Filter Efficiency». MA thesis. The University of Toledo, Nov. 2006.

[48] Yash Gupta, V. Sree Pawan Kumar Reddy, Sunil Shukla, and V. Sai Jayendra. *Design and Fabrication of Air Purifier Using HEPA Filter*. Tech. rep. Capstone project. Lovely Professional University, 2019.

[49] Ruizhe Zhang, Han Han, Guocheng Xu, Yufeng Zheng, and Xiang Li. «Structural Design of HEPA Filter». In: *International Journal of Environmental Research and Public Health* 17.18 (2020), p. 6849. DOI: 10.3390/ijerph17186849. URL: https://pmc.ncbi.nlm.nih.gov/articles/PMC7498897/.

[50] Zhonglin Xu. «Structural Design of HEPA Filter». In: *Fundamentals of Air Cleaning Technology and Its Application in Cleanrooms*. Berlin, Heidelberg: Springer, 2014. Chap. 5, pp. 267–333. ISBN: 978-3-642-39374-7.

[51] Joey Fox. *Clean Air Delivery Rate Is All That Matters!* Oct. 2021. URL: https://itsairborne.com/clean-air-delivery-rate-is-all-that-matters-5a5a064c211e.

[52] Hao Luo and Lexuan Zhong. «Ultraviolet germicidal irradiation (UVGI) for in-duct airborne bioaerosol disinfection: Review and analysis of design factors». In: *Building and Environment* 197 (2021), p. 107852. DOI: 10.1016/j.buildenv.2021.107852.

[53] Edward A. Nardell, Scott J. Bucher, Philip W. Brickner, Charles Wang, Richard L. Vincent, Kathleen Becan-McBride, Mark A. James, Max Michael, and James D. Wright. «Safety of Upper-Room Ultraviolet Germicidal Air Disinfection for Room Occupants: Results from the Tuberculosis Ultraviolet Shelter Study». In: *Public Health Reports* 123.1 (2008), pp. 52–60. DOI: 10.1177/003335490812300109.

[54] Surapong Rattanakul and Kumiko Oguma. «Inactivation kinetics and efficiencies of UV-LEDs against Pseudomonas aeruginosa, Legionella pneumophila, and surrogate microorganisms». In: *Water Research* 130 (2018), pp. 31–37. DOI: 10.1016/j.watres.2017.11.050.

[55] A. H. Al-abdalall, S. A. Al-Dakheel, and H. A. Al-Abkari. «Fungal and bacterial colonization in the A/C filters and ducts». In: *Saudi Journal of Biological Sciences* 28.6 (2021), pp. 3443–3451. DOI: 10.1016/j.sjbs.2021.03.023.

[56] Stephen J. Kemp and Thomas H. Kuehn. «Microbial contamination of building HVAC systems: A review». In: *Journal of the Air & Waste Management Association* 57.12 (2007), pp. 1472–1481. DOI: 10.3155/1047-3289.57.12.1472.

[57] Li Liu, Dandan Wei, Junjie Liu, and Qingyan Chen. «Bioaerosol deposition in ventilation ducts: A review of mechanisms and experimental methods». In: *Building and Environment* 166 (2019), p. 106292. DOI: 10.1016/j.buildenv.2019.106292.

[58] Yuguo Li, Peixian Guo, Hongbo Ren, Yixuan Wang, and Guangyu Cao. «The role of ventilation systems in the transmission of airborne pathogens: Lessons from the COVID-19 pandemic». In: *Building and Environment* 205 (2021), p. 108170. DOI: 10.1016/j.buildenv.2021.108170.

[59] Philip R. Morey and W. G. G. «HVAC systems as reservoirs for microbial growth: A review of the relationship between system hygiene and occupant health». In: *Indoor Air* 10.3 (2000), pp. 259–266. DOI: 10.1034/j.1600-0668.2000.010003259.x.

[60] John Zhang, Doug Huntley, Andy Fox, Bryan Gerhardt, Al Vatine, and John Cherne. «Study of Viral Filtration Performance of Residential HVAC Filters». In: *ASHRAE Journal* (Aug. 2020).